The Astrophysical Journal, 825:78 (18pp), 2016 July 1 doi:10.3847/0004-637X/825/1/78

EMERGING POSSIBILITIES AND INSUPERABLE LIMITATIONS OF EXOGEOPHYSICS: THE EXAMPLE OF PLATE TECTONICS

Vlada Stamenković[1,2] and Sara Seager[3,4]
[1] California Institute of Technology, Department of Geological and Planetary Sciences, Mail Stop 100-23, Pasadena, CA 91125, USA; rinsan@caltech.edu
[2] Jet Propulsion Laboratories, 4800 Oak Grove Drive, Pasadena, CA 91109, USA
[3] Massachusetts Institute of Technology, Department of Earth, Atmospheric, and Planetary Sciences, 77 Massachusetts Avenue, Cambridge, MA 02139, USA; seager@mit.edu
[4] Massachusetts Institute of Technology, Department of Physics, 77 Massachusetts Avenue, Cambridge, MA 02139, USA
Received 2014 December 2; accepted 2016 March 7; published 2016 July 1

ABSTRACT

To understand the evolution and the habitability of any rocky exoplanet demands detailed knowledge about its geophysical state and history—such as predicting the tectonic mode of a planet. Yet no astronomical observation can directly confirm or rule out the occurrence of plate tectonics on a given exoplanet. Moreover, the field of plate tectonics is still young—questioning whether we should study plate tectonics on exoplanets at this point in time. In this work, we determine the limitations and the emerging possibilities of exogeophysics, the science of connecting geophysics to exoplanets, on the example of plate tectonics. Assuming current uncertainties in model and planet parameters, we develop a qualitatively probabilistic and conservative framework to estimate on what kind of planets and where in the Galaxy plate tectonics might occur. This we achieve by modeling how plate yielding, the most critical condition needed for plate mobility and subduction, is affected by directly observable (planet mass, size) or indirectly, to some degree, assessable planet properties (structure and composition). Our framework not only highlights the importance of a planet's chemistry for the existence of plate tectonics and the path toward practical exogeophysics but also demonstrates how exoplanet science can actually help to better understand geophysics and the fundamentals of plate tectonics on Earth itself.

Key words: astrobiology – Earth – planets and satellites: composition – planets and satellites: interiors – planets and satellites: tectonics – planets and satellites: terrestrial planets

1. INTRODUCTION—THE RISE OF PROBABILISTIC EXOGEOPHYSICS

Plate tectonics is a complex geophysical phenomenon, defined dynamically by mantle convection with a predominantly mobile surface, where old plates are constantly returned to the planet interior and new ones are formed. Additionally, plate tectonics is kinematically characterized by specific plate motion geometry on a geoid such as one-sided subduction. It is in contrast to stagnant lid convection where a global rigid plate thermally insulates a planet's interior and does not take part in mantle convection, partially decoupling surface and interior. Throughout this work, we focus on the dynamic aspects of plate tectonics, such as a mobile surface and subduction, which are the major facets of plate tectonics that impact climate and biosphere.

The rocky planets in our own solar system have a broad chemical similarity (e.g., they are dominated by (Mg, Fe) silicates and oxides) but also a great diversity in structure and composition (e.g., iron content). There is no reason to expect that rocky exoplanets have a similar composition and structure to that of Earth. Therefore, we ask how diverse planet conditions impact the likelihood of a rocky planet to initiate and maintain plates and subduction from a dynamic perspective. We specifically address the following questions:

a. Which planets are the optimal candidates for plate tectonics, and which observable properties, if any, characterize such planets? Where are they in our Galaxy?
b. What are the insuperable limits to exogeophysics? How can we use exogeophysics to improve our knowledge of the fundaments of geophysics here on Earth?

The processes driving plate tectonics are complex and associated with uncertainties, which we will discuss in the next sections. We are aware of these uncertainties and carry them along while forming a general, though evolving, framework, toward computing the likelihood of plate tectonics as a function of planet mass, composition, structure, initial conditions, planet location in the Galaxy, and a planet's host star. Our goal is to show what questions regarding plate tectonics on exoplanets we can answer today (in spite of uncertainties; see Section 3.1), what we will be able to do once we have reduced the associated model uncertainties (Sections 3.2–3.7; and for the current most likely set of parameters see Section 4.1), and what questions we will likely never be able to answer unless we set foot on the studied exoplanet (Section 4.2).

1.1. Motivation—Fundamental Impact on Climate, Biosignatures, and Life

The tectonic mode of a planet impacts outgassing and surface environments. Understanding how planet conditions influence the tectonic mode of a planet is thus needed to understand the long-time evolution of life and climate on Earth and beyond. Moreover, from an astronomical observational perspective, the tectonic mode matters when searching for signs of alien life: the atmospheric composition and biosignature gases (gases associated with life that accumulate in a planet's atmosphere; e.g., Seager et al. 2013) on alien worlds as a function of time are affected by the tectonic mode of the planet. Therefore, connecting planetary properties that can be either directly observed or indirectly estimated (e.g., planet mass, average density, structure, concentration of radiogenic heat sources, and Fe/Mg ratio of the mantle) to a probability of plate

tectonics occurring on that planet will help us to better understand biosignature gases, the climate, and the potential of surface life.

Furthermore, by exploring how diverse planetary conditions impact the initiation and maintenance of plate tectonics, we are also forced to investigate the fundamental drivers of planet evolution.

Also encouraging for the field of exogeophysics are rocky Earth-sized planets recently discovered around Trappist-1 (Gillon et al. 2016) and hot rocky super-Earths like 55 Cnc e (Demory et al. 2016), which might allow insight into geodynamic processes on rocky exoplanets.

1.2. Plate Yielding, Stresses, and Uncertainties

1.2.1. The Importance of Plate Yielding for Plate Tectonics

We showed in Stamenković & Breuer (2014) that by coupling a 1D thermal evolution model with a plate yielding model, we can explain major trends observed with 2D or 3D numerical experiments studying the behavior of "plate-tectonics-like" mantle convection (e.g., Stein et al. 2004, 2011, 2013; O'Neill & Lenardic 2007; Van Heck & Tackley 2011; Foley et al. 2012; Noack & Breuer 2014; Stamenković et al. 2016). Generally, in such 2D or 3D models, "plate-tectonics-like" mantle convection with mobile plates and subduction occurs when the driving stress deforming plates τ_D, caused by mantle convection, exceeds the yield stress of lithospheric plates, τ_y (Figure 1). The driving stress τ_D corresponds to the second invariant of the deviatoric stress tensor (e.g., Moresi & Solomatov 1998).

Therefore, like in many 2D and 3D models (e.g., Moresi & Solomatov 1998; Trompert & Hansen 1998; Tackley 2000; Stein et al. 2004), we focus on plate yielding as the critical aspect of plate tectonics in order to map out the necessary conditions for plate tectonics to occur.

1.2.2. The Emergence of Two Thermodynamic Scenarios for Plate Yielding

The thermal evolution and plate yielding model depends on three parameters and the stress type that is causing plate failure (see Section 2 and Appendix C for all details). Specifically, we need the Nusselt–Rayleigh scaling parameter $\beta \in [1/5, 1/3]$ that describes the cooling efficiency of the planet, a parameter $\gamma \in [2/5, 2/3]$ that describes convective velocity, and a parameter $\varepsilon \in [0, 1/6]$ that describes plate length as a function of Rayleigh number, which is a measure of convective vigor. The driving stress τ_D causing plate failure can be dominated by surface normal stresses ($\tau_D = \tau_{zz}$) or shear stresses ($\tau_D = \tau_{zx}$) at the plate base (see Figure 1(a)).

We showed in Stamenković & Breuer (2014) that depending on the specific choice of model parameters (β, γ, ε), which are not precisely known, and as a function of whether surface normal stresses ($\tau_D = \tau_{zz}$) or shear stresses at the plate base ($\tau_D = \tau_{zx}$) drive plate failure, two distinct thermodynamic behaviors of plate tectonics, which we named $\chi_{\rm low}$ and $\chi_{\rm high}$, emerged. The distinction between the $\chi_{\rm low}$ and the $\chi_{\rm high}$ scenarios lies in whether plate yielding is more likely with decreasing or increasing interior temperatures, all other planet conditions remaining the same. When enough heat sources are present for vigorous convection, then for $\chi_{\rm low}$ plate failure is less likely for a hotter planet. For $\chi_{\rm high}$, we found that plate yielding is more likely for a hotter planet. All parameters, equations, and how model parameters relate to $\chi_{\rm low}$ or $\chi_{\rm high}$ are described in great detail in Section 2, Appendix C, and Figure 1 and are explicitly derived in Stamenković & Breuer (2014).

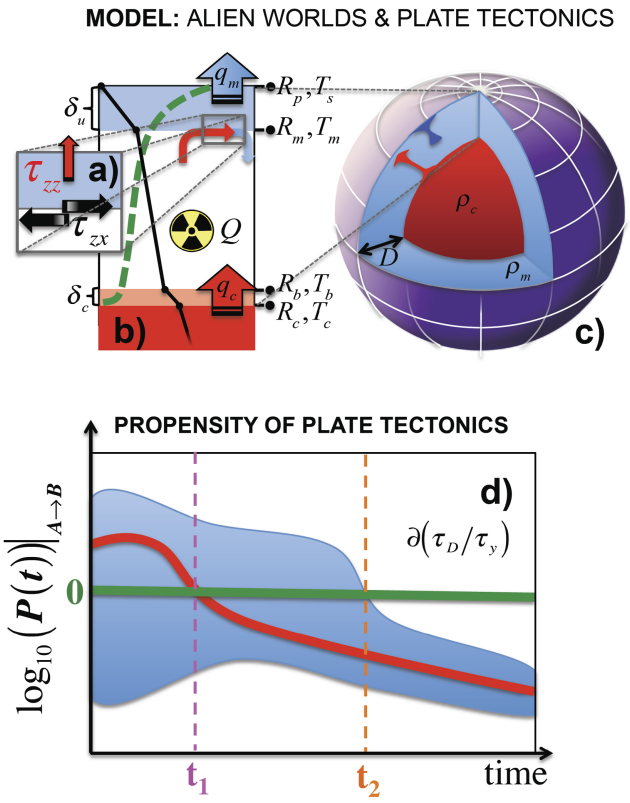

Figure 1. Model illustrated for maintenance of plate tectonics. (a) Plate yielding: driving stresses τ_D must overcome yield stresses τ_y. Driving stresses are either basal shear $\tau_D = \tau_{zx}$ or normal stresses $\tau_D = \tau_{zz}$. (b) Thermal model: R is the distance from the center of the planet outward, and T is temperature. Cold and hot thermal boundary layers (δ_u, δ_c) drive convection and heat fluxes through mantle and core (q_m, q_c). Primordial heat and decaying heat sources $Q(t)$ warm the mantle of convective depth D. The depth profiles of temperature (solid black line; adiabatic outside the thermal boundary layers and linear within them) and viscosity (dashed green line) for temperature-dependent viscosity are shown. (c) Planet model: we vary core-to-planet mass fraction from 0 to 0.65 for coreless to Mercury-structured planets. We use average values for mantle and core, e.g., average densities (ρ_m, ρ_c) except for the viscosity. (d) Propensity of plate tectonics $P(t)$: a change of a planet property from A to B (like increased core size) can lead for a family of planets (like for an Earth-sized planet with varied composition) to a phase space defining all the propensity of plate tectonics evolution curves for the family of planets (in blue). In red we highlight the propensity of plate tectonics for a specific planet (like Earth). Therefore, a change from A to B decreases for the whole planet family the propensity of plate tectonics after the time t_2; for Earth, the same change decreases the propensity of plate tectonics already after the time t_1. We are looking for robust results, where a change from A to B at all times leads to positive or negative values for $\log_{10}P$.

1.2.3. The End of the "Plate Tectonics Wars"

During the past decade, there have been many publications on the subject of plate tectonics on massive rocky planets (e.g., O'Neill & Lenardic 2007; O'Neill et al. 2007; Valencia et al. 2007; Korenaga 2010; Stein et al. 2011, 2013; Van Heck & Tackley 2011; Foley et al. 2012; O'Rourke & Korenaga 2012; Stamenković et al. 2012; Noack & Breuer 2014; Stamenković & Breuer 2014). Associated with these papers was a vivid debate, casually given the name "plate tectonics wars" by a magazine article in *Astronomy Now*, on whether super-Earths would allow for plate tectonics to occur or not (Chorost 2013). All these previous studies looked mainly at how plate yielding

Table 1
Parameters

Variable	Physical Meaning	Value	Units	References
$M_{\oplus}$	Earth mass	5.974×10^{24}	kg	1
$T_{S,\oplus}$	Mean Earth surface temperature	288	K	...
$R_{p,\oplus}$	Mean Earth planetary radius	6371	km	1
$R_{c,\oplus}$	Mean Earth core radius	3480	km	1
$f_{c,\oplus}$	Earth core-to-planet mass fraction	0.3259	...	1
$k_{m,\oplus}$	Average Earth mantle thermal conductivity	4	$Wm^{-1}\,K^{-1}$	2
$\alpha_{m,\oplus}$	Average Earth mantle thermal expansivity	2×10^{-5}	K^{-1}	2
$E_{\oplus}$	Earth mantle rock activation energy	300	$kJ\ mol^{-1}$	3
$T_{\rm ref}$	Reference temperature for viscosity	1600	K	3
$\eta_{\rm ref,\oplus}$	Earth mantle reference viscosity	10^{21}	Pa s	3
$\mathrm{Ra}_{\rm crit}$	Critical Rayleigh number	1000	...	1
$C_{m,\oplus}$	Average Earth mantle heat capacity	1250	$J\,kg^{-1}\,K^{-1}$	3
$C_{c,\oplus}$	Average Earth core heat capacity	800	$J\,kg^{-1}\,K^{-1}$	4
$C_{\rm fric,\oplus}$	Average Earth-like lithospheric friction coefficient	0.15	...	5
$\rho_{\rm up,\oplus}$	Average Earth lithospheric density	3500	$kg\ m^{-3}$	1
	Mass–Radius Scaling Parameters for Varied Planet Structures			
$(a, b, \phi, \psi)_{\rm EL}$	For Earth-like structure	1, 1, 0.27, 0.247	...	6, 7
$(a, b, \phi, \psi)_{\rm SM}$	For Mercury-like structure	0.915, 1.26, 0.3, 0.3	...	6, 7
$(a, b, \phi, \psi)_{\rm CL}$	For coreless structure	1.05, 0, 0.28, 0	...	6, 7

Note. Standard parameters: (1) Turcotte & Schubert (2002), (2) Stevenson et al. (1983), (3) Stamenković et al. (2011), (4) Buffett et al. (1996), (5) Escartin et al. (2001), (6) Seager et al. (2008), (7) Valencia et al. (2006).

efficiencies change with an increasing planet mass similar to our model here. More massive planets are generally hotter, and hence we concluded in Stamenković & Breuer (2014) that the question of plate tectonics for rocky super-Earth models directly relates to the question whether plate tectonics is more or less likely for a hotter planet interior. This allowed us to resolve the previous debate by mainly relating the discrepancies of the past decade to some of the groups choosing 1D model parameters falling within the $\chi_{\rm low}$ scenario and some within the $\chi_{\rm high}$ scenario and to disagreeing 2D models scaling interior heat differently with planet mass.

1.2.4. Which Thermodynamic Scenario Is Realistic?

What remains unanswered is which thermodynamic scenario, $\chi_{\rm low}$ or $\chi_{\rm high}$, is more likely in nature. We have previously shown that the question whether $\chi_{\rm low}$ or $\chi_{\rm high}$ is more likely is tightly related to the type of stresses driving plate failure and subduction for the initiation and maintenance of plate tectonics (Stamenković & Breuer 2014; Stamenković et al. 2016): for appropriate values of 1D model parameters (β, γ, ε), we found that generally for shear stresses driving plate failure from the plate base upward ($\tau_D = \tau_{zx}$) $\chi_{\rm low}$ is the resulting thermodynamic scenario. For the classic picture where normal stresses drive plate failure from the surface downward ($\tau_D = \tau_{zz}$ and a standard value of $\varepsilon \sim 0$), we found that instead $\chi_{\rm high}$ is much more likely for most values of (β, γ).

To test which stresses initiate the formation of plates and subduction (hence whether $\chi_{\rm low}$ or $\chi_{\rm high}$ is more likely for the initiation of a "plate-tectonics-like" mode of convection), we recently performed 3D time-dependent spherical mantle convection experiments in the episodic mode with CitcomS (Stamenković et al. 2016), based on the methods derived in Höink et al. (2012), to gain some insight into a causal, time-dependent, far-from-equilibrium perspective on the stresses initiating the transition from stagnant lid to mobile lid with mantle overturn events. This is an extension of older models focusing only on steady state stagnant lid convection, where the time dependence of stresses is minimized (e.g., Van Heck & Tackley 2011; Foley et al. 2012; Wong & Solomatov 2015). We found that the classic scenario of normal stresses governing the transition from stagnant lid to plate tectonics (and hence $\chi_{\rm high}$) is questionable for the initiation of plate tectonics from a time-dependent stress point of view and that possibly shear stresses could be driving plate yielding bottom up from the plate base toward the surface. This could make the $\chi_{\rm low}$ scenario more likely to describe the initiation of plate tectonics. The dominance of $\chi_{\rm low}$ for the initiation and maintenance of plate tectonics on planets as massive as or more massive than Earth is also supported by Stamenković & Breuer (2014).

Although the results based on the new approach in Stamenković et al. (2016) for modeling the initiation of plate tectonics are interesting, we still need additional time-dependent 3D convection experiments with more realistic boundary conditions and model parameters, as well as more fundamental thermodynamic work, including melt generation and transport, in the episodic and plate tectonics modes to be capable of understanding how shear or normal stresses precisely and time-dependently impact the initiation and maintenance of plate failure, mobility, and subduction. Until then, although our own current 3D time-dependent initiation results and a comparison with 2D maintenance models suggest that $\chi_{\rm low}$ is more realistic for both initiation and maintenance of a "plate-tectonics-like" mode of convection, it indeed remains an open question whether $\chi_{\rm low}$ or $\chi_{\rm high}$ (or a combination of both depending on planet properties) is appropriate for real planet interiors.

1.3. A Trend-based Framework toward Exogeophysics

Bearing the unknown predominance of $\chi_{\rm low}$ versus $\chi_{\rm high}$ for planet interiors, we develop a general framework by studying how plate failure is affected by planet composition, mass, and

structure assuming wide planet initial condition thresholds for both $\chi_{\rm low}$ and $\chi_{\rm high}$ scenarios. With this we try to create an unbiased framework, whose results can be continuously reinterpreted with our evolving knowledge about how shear and normal stresses impact the initiation and maintenance of plate tectonics as a function of time. In the Discussion section, we would like to provide our current best estimates for the occurrence of plate tectonics across the Galaxy, assuming the currently favored $\chi_{\rm low}$ scenario.

We focus on planet properties, which to some degree can be directly or indirectly (as we discuss later) estimated, such as the planet's mass, radiogenic heat and iron mantle content, the core-to-planet mass fraction, and whether a planet is differentiated or not. The effects of water and surface temperature are left for future work, as their interaction with mantle convection is even more complex than the processes studied here.

We do not compute quantitative probabilities, but qualitative trends instead. This approach allows a start to mapping out the phase space for worlds that are more or less likely to support a "plate-tectonics-like" mode of convection—which is already of great importance not only for exoplanet science but also to fundamental geophysics.

2. MODEL SUMMARY

To prevent repetition, we give a brief overview of our planet, plate tectonics, and thermal evolution model (see Figure 1). In Appendix C, we provide additional model details, list the used scaling laws, and explain the choice of parameters used to model diverse planet interior compositions for the interested reader. Additionally, we refer to Stamenković & Breuer (2014) and to Stamenković et al. (2012) for a detailed description of the complete model, in-depth robustness tests, comparison with 2D, and precise derivations of all used scaling laws and the boundaries for the range of values of the model parameters β, γ, and ε.

Our 1D thermal history and plate tectonics model does not capture lateral variability, but it is suited to unveil trends and to simulate in a reasonable time a variety of planets for realistic parameters (like realistically high initial temperatures for planets more massive than Earth >8000 K, which cannot yet be numerically handled with most 2D or 3D models). Our 1D model compares well with the results from time-dependent 2D planet interior evolution models (using the spherical code GAIA; Hüttig & Stemmer 2008; see Stamenković et al. 2012), 2D "plate-tectonics-like" convection models (in Stamenković & Breuer 2014), and 3D experiments for the initiation of plate tectonics in dynamic disequilibrium (see Stamenković et al. 2016).

2.1. Thermal Evolution and Plate Yielding

Our thermal evolution model describes how heat flows through a planet's interior, and our plate tectonics model describes how the effectiveness of plate yielding changes during the planet's thermal history. Here we model evolution over 13 Gyr (~the age of the universe), allowing planets to be of any age between 0 and 13 Gyr. We model the energetic evolution of planet interiors with a classic boundary layer model, which we have previously extended to allow a wide range of thermal and transport properties to be used (Stamenković et al. 2012).

2.1.1. Thermal Evolution

Our time-dependent boundary layer model consists of two thermal boundary layers (δ_u, δ_c) in the upper and lower mantle, respectively, which represent cold upper and hot lower mantle instabilities that drive convection, which is the dominant heat transport mechanism in most planetary mantles (illustration in Figures 1(b) and (c)). The boundary layers are used to parameterize the heat fluxes out of the mantle and out of the core (q_m, q_c), driven by primordial heat and decaying radiogenic mantle heat sources Q, as a function of time. The heat fluxes are coupled to classic energy conservation in the mantle and core (Stevenson et al. 1983; Grott & Breuer 2008) generalized for a wide range of thermal and transport properties (Stamenković et al. 2012). Together, the boundary layer model and energy conservation allow deriving the evolving interior temperature profiles within a rocky planet as a function of time after specifying an initial temperature profile. The initial temperature profile ranges from cool adiabatic ("cool") to hot temperatures along the mantle "solidus" ("hot" scenario, not to be confused with modeling a magma ocean). We assume vigorous mantle convection, so that the thermal profile is adiabatic between the thermal boundary layers.

The viscosity, η, controls the thermal evolution and is temperature- and pressure-dependent (the latter only for an effective activation volume $V^*_{\rm eff} > 0$):

$$\eta(P, T) = \eta_{\rm ref} \exp\left(E^* R_g^{-1}(T^{-1} - T_{\rm ref}^{-1}) + (R_g T)^{-1} P \times V^*_{\rm eff}(P)\right). \quad (1)$$

The Arrhenius-type form for the viscosity in Equation (1) is a result of creep being a temperature-activated process (see Stamenković & Sohl 2015). In Equation (1), T [K] and P [Pa] are temperature and pressure, respectively, the universal gas constant is $R_{\rm g} \sim 8.3145\,{\rm J K^{-1}\,mol^{-1}}$, ($T_{\rm ref}$, E^*) are reference temperature and activation energy of mantle rock, and $V^*_{\rm eff}$ is the effective activation volume defining the pressure dependence of the viscosity (see Stamenković et al. 2011 for details and Table 1 for parameter values). For rocky super-Earths, our plate tectonics model currently only allows us to make approximate predictions when $V^*_{\rm eff} \gg 0$ (Appendix B.2). Thermal properties, such as the mantle thermal conductivity k_m, expansivity α_m, and heat capacity C_m, are, after the mantle viscosity, of secondary importance, and average values are used (see Stamenković & Breuer 2014).

The surface boundary conditions for modeling the thermal history of planets with plate tectonics and with stagnant lid convection differ from each other: for a planet in a "plate-tectonics-like" mode of convection, the upper thermal boundary layer connects to the planet surface, whereas for stagnant lid convection, the upper thermal boundary layer is below a stagnant lid, which is described by a conductive growth equation (Grott & Breuer 2008). For maintenance, we assume "plate-tectonics-like" mantle convection and study how easily plate yielding is maintained. For initiation, we assume stagnant lid convection and study how easily plate yielding initiates.

We obtain similar results for initiation and maintenance when studying the effects of bulk mantle properties on plate yielding. Therefore, although we run maintenance and initiation cases, we illustrate only our maintenance framework.

2.1.2. Plate Yielding—a First Crucial Step toward Plate Tectonics

To model the effectiveness of plate yielding, we define a failure function X, which must exceed unity to allow plate tectonics to operate:

$$X(M,\, t,\, T_0,\, T_s,\, \text{composition},\, \text{structure},\, \chi) = \tau_D/\tau_y > 1. \quad (2)$$

This failure function X depends on planet mass M, planet age t, initial conditions T_0, surface temperature T_s, composition, structure, and especially a thermodynamic parameter χ. The critical parameter χ is a combination of the thermal model's Nusselt–Rayleigh parameter for the heat flow β, the convective velocity parameter γ, the plate length parameter ε, and whether the driving stress τ_D is controlled by basal shear stresses or normal stresses close to the surface: we call the basal shear stress scenario ($\tau_D = \tau_{zx}$) the F model (for *fundus*, Latin word for "base") with $\chi_F = \beta + \gamma$; we call the normal stress scenario ($\tau_D = \tau_{zz}$) the S model (for *superficie*, Latin word for "surface"), as normal stresses are mainly large close to the surface (Solomatov 2004; Stamenković et al. 2016) with $\chi_S = 2\beta + \gamma - \varepsilon$ (derivation in Stamenković & Breuer 2014).

We find that the qualitative nature of how the effectiveness of plate yielding reacts to planet mass, composition, and structure is approximately controlled by how plate yielding reacts to a change of interior heat, as any bulk property change ultimately affects the planet's interior heat budget. We find two thermodynamic scenarios described with $\chi < \chi_{\text{crit,dyn}}$ (χ_{low} model, plate yielding less effective for hotter planets, all other properties remaining the same) and $\chi > \chi_{\text{crit,dyn}}$ (χ_{high} model, plate yielding more effective for hotter planets, all other properties remaining the same) by demanding that for χ_{low} we must have $\partial X/\partial \Delta T < 0$ and that for χ_{high} we must have $\partial X/\partial \Delta T > 0$ for an interior temperature change ΔT. The critical parameter $\chi_{\text{crit,dyn}}$, determining the transition between χ_{low} and χ_{high}, is computed by demanding that $\partial X(\chi = \chi_{\text{crit,dyn}})/\partial \Delta \text{T} = 0$. For maintenance of plate tectonics, this leads to $\chi_{\text{crit,dyn}}(t) = [1 + R_g \cdot (T_s + \Delta T)^2/\Delta T \cdot E^*]^{-1}$ (Stamenković & Breuer 2014). For initiation, the critical factor must be numerically computed.

We therefore study plate yielding as a function of χ_{low} versus χ_{high}. We can choose any arbitrary values of (β, γ, ε) for the F or S model to illustrate our results falling within either χ_{low} or χ_{high}, as any value of $\chi \in \chi_{\text{low}}$ (or $\chi \in \chi_{\text{high}}$) leads to the same qualitative results for how the propensity of plate tectonics depends on a planet condition. We choose two reasonable and commonly used parameter sets to illustrate our results (see boundaries for (β, γ, ε) in Appendix C), which are ($\beta = 1/5$, $\gamma = 2/5$, F) representing χ_{low} and $\left(\beta = \frac{1}{3}, \gamma = \frac{2}{3}, \varepsilon = 0, S\right)$ representing χ_{high}. We show in the discussion and in Appendix C also evolution curves for other parameters falling within the χ_{low} scenario, such as ($\beta = 0.3$, $\gamma = 0.4\overline{3}$, F), to illustrate how the explicit choice of parameters within each thermodynamic scenario does not affect the qualitative plate-tectonics-related results.

Ideally, we would check whenever the failure function $X > 1$ to decide whether plate tectonics is possible. However, the constants necessary to compute X are too uncertain. Instead, we compute an effectiveness of plate yielding as a function of χ_{low} or χ_{high} and name it the propensity of plate tectonics $P(t)$ (see Figure 1(d)). To illustrate our results, we focus on three representative propensity functions:

$$P_{\text{Div}}(M,\, \text{Div},\, t) = X(M,\, \text{Div},\, t)/X(M,\, t), \quad (3)$$

$$P_M(M,\, t) = X(M,\, t)/X(M = 1,\, t), \quad (4)$$

$$P_{M,\text{Div},\oplus}(M,\, \text{Div},\, t) = X(M,\, \text{Div},\, t)/X(M = 1,\, \oplus,\, t). \quad (5)$$

1. *The effects of diversity alone:* P_{Div} (Equation (3)) describes how the drivers for plate tectonics of an arbitrary rocky planet of relative mass M change when composition or structure is altered (symbolized with "div" for "diversity").
2. *The effects of mass alone:* P_M (Equation (4)) describes how the drivers for plate tectonics react to an increase of relative mass alone (shown from $M = 1$ to M) for an arbitrary rocky planet while all other planet properties (structure, composition) remain the same.
3. *In relation to Earth:* $P_{M,\text{Div},\oplus}$ (Equation (5)) describes how the drivers for plate tectonics change when planet mass, structure, and composition are altered in relation to our Earth model.

We illustrate our results by plotting the decimal logarithm of $P(t)$, $\log_{10}(P)_{A\to B}$ for a change of planet condition from A to B (like increase in planet mass, so $\log_{10}(P_M)$), which can have arbitrary positive and negative values. Positive (negative) values of $\log_{10}(P)_{A\to B}$ indicate that the change of condition from A to B increased (decreased) the propensity of plate tectonics.

2.2. Planet Diversity

In the following, we summarize the studied variations in planet composition, structure, mass, and initial temperature conditions. See Table 1 for Earth reference values and mass-radius scaling parameters. We have provided in Appendix C.3 a detailed summary of (1) the mass–radius scalings, (2) experimental data and ab initio calculations on material properties (reference viscosity, activation energy, thermal conductivity, thermal expansivity, heat capacity), and (3) estimates on the natural variability in planet composition based on the evolution of the interstellar medium (ISM)—which we needed to select the parameter values in order to model the different planet compositions and structures described below.

We ran ~80,000 simulations to investigate how the propensity of plate tectonics depends on variations of

1. mantle composition (radiogenic heat source concentration (U, Th, K) 0.1–10 times the Earth reference value, varied Fe, Mg, SiC content);
2. structure (from coreless to Mercury structure corresponding to a core-to-planet mass fraction of $f_c = 0$–0.65);
3. planet mass (1–10 Earth masses corresponding to $M = 1$ −10 in relative Earth mass units); and
4. initial conditions (from mantle solidus ("hot" or molten scenario) to adiabatic ("cool" scenario) temperatures). The surface temperature is varied between current Earth-like and current Venus-like temperatures.

The motivation for such a broad parameter space lies in our goal of determining which "plate-tectonics-related" conclusions are robust for a large family of planets.

Within this large family of planet conditions, we distinguish two distinct classes: silicate and carbon planets. Silicate planets

are rocky planets as found in our own solar system, where rock is composed of oxygen-dominated silicates and oxides (∼(Mg, Fe)SiO and (Mg, Fe)O). On the other hand, carbon planets (as introduced by Kuchner & Seager 2005) have been hypothesized to orbit stars with initially large C/O ratios where silicates and minerals like periclase and wüstite are replaced with silicon-carbide (SiC, in Earth or in meteorites occurring as the rare moissanite mineral), graphite, or, at higher pressures, diamond. Although there is so far no evidence that such planets exist (except for the hypothesis that 55 CnC e might be a carbon planet; see Madhusudan et al. 2012), it is helpful to account for their possibility—especially if we bear in mind how much exoplanet science has so far surprised us. Therefore, we focus on silicate planets as the possibly today most likely planets in the Galaxy but we also investigate the contrasting evolution of carbon-rich and pure carbon planets, and discuss implications for planets that might have compositions between these two types.

3. RESULTS—A PLATE YIELDING FRAMEWORK WITH UNCERTAINTIES

We ran ∼80,000 simulations for 1, 3, 5, and 10 $M_{\oplus}$ planets mimicking different compositions, structures, and initial conditions for $\chi_{\rm low}$ and $\chi_{\rm high}$, maintenance, and initiation. We illustrate how an increase in a specific planet property impacts the decimal logarithm of the propensity of plate tectonics, $\log_{10}(P)$. Positive (negative) values of $\log_{10}(P)$ indicate that the change supports (suppresses) the occurrence of plate tectonics from a plate yielding perspective. Additionally, we show in Appendix A how variations in thermal and transport properties impact the propensity of plate tectonics, and in Appendix B.1 we show how an inclusion of melt generation and extraction does not qualitatively affect our conclusions.

3.1. Robust Results

Generally, all results depend strongly on the thermodynamic χ scenario and often lead to contradicting conclusions between $\chi_{\rm low}$ and $\chi_{\rm high}$ models, as we show in Figure 2, where we illustrate the results of our complete framework. Figure 2 is a guideline for understanding what kinds of planets are more or less supportive of plate tectonics from a plate yielding perspective and how better constraints on composition and initial state can lead to more robust results. The only robust results for the propensity of plate tectonics independent of χ are the following:

1. Without knowing initial interior temperatures and planet composition or structure, plate tectonics could be less or more likely on rocky super-Earths than on Earth.
2. Iron-rich mantle rock reduces the propensity of plate tectonics for silicate planets that form molten.
3. Carbon planets are generally not ideal candidates for plate tectonics (with some exceptions for $\chi_{\rm low}$; see Section 3.6). This is because of the significantly greater thermal conductivity and viscosity of carbon-rich mantle rock, which can lead to problems in maintaining vigorous mantle convection over geologically long times.

Even for a specific χ scenario many results are nonunique without knowing planet composition and initial condition (mixed colors are common in Figures 2(a) and (b)). This is due to the large parameter range assumed for the viscosity, activation energy, and initial conditions—which stretch the space of possible thermodynamic responses to interior property changes.

However, being highly likely that all planets form molten (e.g., Breuer & Moore 2015) and bearing in mind that there is no observational evidence for the existence of carbon planets yet opens up the possibility that silicate planets like the rocky planets in our solar system are the prevalent compositional kind of planets in the whole Galaxy.

For such silicate planets starting along the mantle solidus, the results become more unique owing to generally lower viscosities allowing a faster self-regulation of the planet interior heat budget (see as well Figure 3), which leads to the rather unambiguous results shown in Figures 2(c) and (d). Therefore, Figures 2(c) and (d) could be the most appropriate representation for all rocky planets in the Galaxy.

Assuming the validity of the $\chi_{\rm low}$ model would make Figure 2(c) currently the best framework to describe how planet conditions impact the propensity of plate tectonics, where a greater planet mass, a greater concentration of radiogenic heat sources and iron in the planet's silicate or oxide mantle, and a lack of core or mantle differentiation reduce the propensity of plate tectonics. For $\chi_{\rm high}$ and initially molten silicate planets, all propensity results are contrary to $\chi_{\rm low}$, with the exception of the impact of the mantle iron content.

We now focus on specific changes in planet condition and how they impact the propensity of plate tectonics as a function of the two thermodynamic scenarios.

3.2. Radiogenic Heat Content and Plate Yielding

Increasing radiogenic heat source concentrations (Q in [W kg^{-1}]) contributes to heating the planet's interior. Therefore, depending on χ, the propensity of plate tectonics increases or decreases significantly with greater Th, U, and K contents. The degree of the propensity being affected by varied Q is almost independent of planet mass (see Figures 3(c) and (f)).

For $\chi_{\rm low}$, the propensity of plate tectonics significantly decreases with an increased concentration of radiogenic substances for any planet. This is due to the strong decrease of upper mantle viscosities caused by increasing heat sources, which significantly reduce the convective shear stresses (see also Section 4.1.2 for limits to this behavior). In contrast, we find for $\chi_{\rm high}$ systems that a higher amount of radiogenic heat sources increases the propensity of plate tectonics. This is because higher interior temperatures increase convective velocities, which control the propensity of plate tectonics for $\chi_{\rm high}$.

3.3. Iron-rich Planet Mantle and Plate Yielding

For initially "hot" silicate planets (starting along the mantle solidus), iron-rich mantle rock reduces the propensity of plate tectonics, independently of χ (see Figures 3(b) and (e)); this is valid for all studied rocky planets for $\chi_{\rm low}$: iron-rich mantle rock weakens the mantle rheology and reduces melting temperatures (see Appendix C.3.2.2). These two effects combined reduce viscosities but also allow faster cooling: for $\chi_{\rm low}$ the melting point reduction does not suffice to compensate the rheological effects, and smaller viscosities reduce driving stresses and the propensity of plate tectonics;

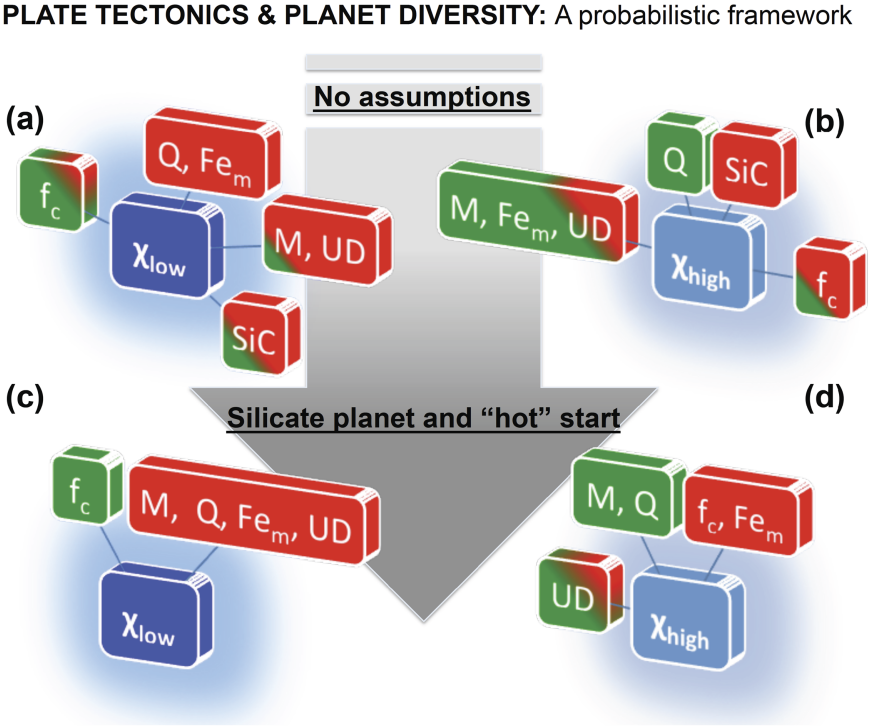

Figure 2. Illustration of how planet mass, composition, structure, initial conditions, and differentiation impact the propensity of plate tectonics for planets as massive or more massive than the Earth, with core mass fractions varying from 0 (coreless) to 0.65 (Mercury-structured), initial radiogenic heat contents from 0.1 to 10 times the Earth reference value, and a variable iron and carbon mantle content, for $\chi_{\rm low}$ and $\chi_{\rm high}$: (a, b) with no restrictions on composition and initial conditions, and (c, d) focusing on silicate planets that formed molten. Red (green) represents that an increase in the specific property always decreases (increases) the propensity of plate tectonics. Intermediate colorings indicate that the effects on the propensity of plate tectonics are nonunique and depend on specific conditions (the degree of increasing/decreasing the propensity of plate tectonics is illustrated with the ratio of green/red shading). The abbreviations are M for planet mass, Fe$_m$ for the concentration of mineralogically bound iron and Q for the concentration of radiogenic heat sources in the mantle, f_c for the core-to-planet mass fraction, SiC for carbon planets in relation to silicate analogs, and UD for undifferentiated planets in relation to differentiated analogs. Shown trends are identical for initiation and maintenance.

for $\chi_{\rm high}$ systems, the same changes generally increase the propensity of plate tectonics—with the exception of silicate planets of any size starting off "hot," where, thanks to the moderate viscosities, the mantle effectively cools and reduces convective stresses.

3.4. Planet Structure and Plate Yielding

A change in planet structure impacts the mantle thickness D, as well as the mantle and core heat fluxes. We find that, although planet structure does not always provide a unique and robust fingerprint for the propensity of plate tectonics, for small planets (but still $M > 1$) and for silicate planets of any mass greater than Earth starting "hot," larger core-to-planet mass fractions f_c increase the propensity of plate tectonics for $\chi_{\rm low}$ (opposite behavior for $\chi_{\rm high}$); see Figures 3(a) and (d). This complex behavior is explained in the following paragraphs: applying the individual mass–radius scalings for a 10 $M_\oplus$ coreless rocky super-Earth and super-Mercury (Equations (17)–(20)) shows that their planetary radii, mantle densities, and gravities vary by less than 15% in relation to the Earth-like-structured $M = 10$ planet (effects are smaller for less massive planets). The major change between the non-Earth-like-structured and Earth-like-structured planets is the mantle depth, which varies by a factor of ∼2.5 for 10 $M_\oplus$ super-Mercuries and coreless super-Earths in relation to an Earth-like-structured super-Earth. This change in mantle thickness additionally modifies the radiogenic mantle and core heat fluxes (the relative radiogenic mantle heat flux decreases for larger f_c and scales approximately with $\sim D$; see Stamenković et al. 2012; the core heat flux increases with f_c). Specifically, for less massive planets or silicate planets that start "hot," heat reservoir differences between different structures have minimal impact on the propensity of plate tectonics owing to lower viscosities and hence a quicker self-regulation. In this case, the failure function scales mainly with changes in mantle thickness ($X \propto D^{3(\chi-1)}$; see Appendix C.2). This leads roughly to a greater propensity of plate tectonics on super-Mercuries for $\chi_{\rm low}$ and on coreless planets for $\chi_{\rm high}$. This result is approximately but not generally valid once we release the constraint on planet composition and initial conditions for more massive planets, as dynamic contributions become important.

Note that we have only explored f_c values below 0.65. We can expect that for greater values of f_c there will be a point where mantle convection will start to cease. For $\chi_{\rm low}$, this would lead to a turnover point where the propensity of plate tectonics would start to decrease for greater values of f_c. However, as shown in Section 3.6, Figure 4, and especially Figure 5, we find no evidence for such a turnover point being within our studied parameter space.

3.5. Undifferentiated Planets and Plate Yielding

We find that undifferentiated planets (planets with no core because metals did not separate from the rocky mantle into a metallic core) have generally a lower propensity of plate tectonics for $\chi_{\rm low}$ than their differentiated counterparts. For the $\chi_{\rm high}$ model, the situation is not as clear as for $\chi_{\rm low}$, but we find roughly the opposite behavior (see Figure 2).

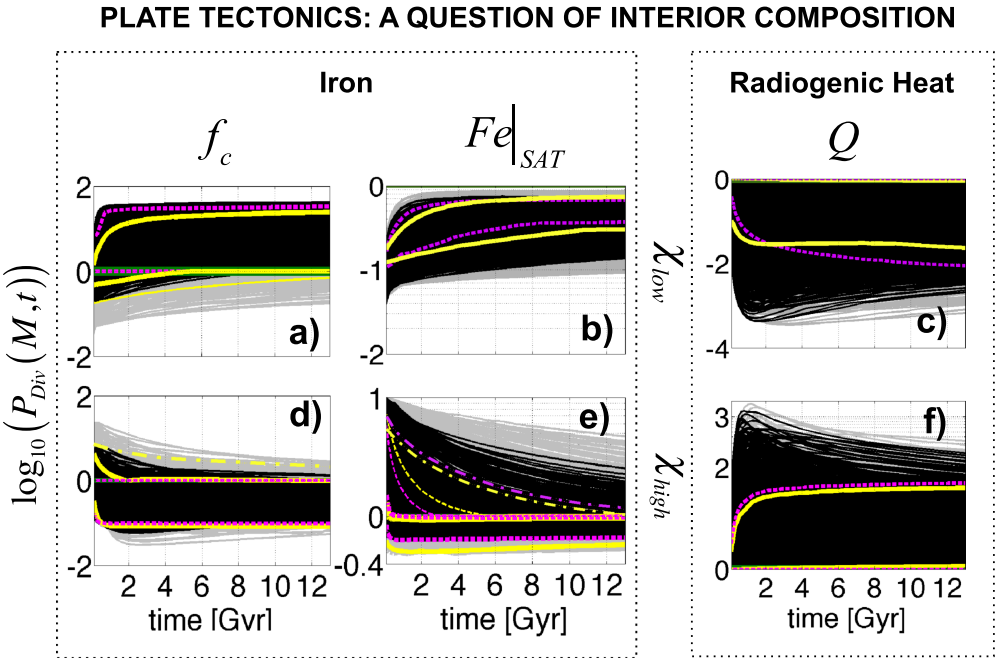

Figure 3. Effects of an increased concentration of mineralogically bound iron and radiogenic heat sources Q within the bulk mantle, and of an increasing core-to-planet mass fraction f_c on the propensity of plate tectonics for $\chi_{\rm low}$ and $\chi_{\rm high}$ (for values of planet mass, composition, and structure within the limits of our specified parameter space in Appendix C.3). Results are shown for $M = 1$ (black) and $M = 10$ (gray) assuming all specified maximal variation in initial conditions, structure, and composition. In (c) and (f) the initial radiogenic heat concentration increases from 0.1 to 10 times the initial Earth reference value (steps of 0.1, 0.2, 1, 5, 10); in (a) and (d) the core mass fraction f_c increases from ∼0 to 0.65 (steps of 0, 0.05, 0.15, 0.3259, 0.45, 0.65); in (b) and (e) we compare Fe- with Mg-silicate-dominated planets—intermediate magnesium numbers lead to intermediate propensities. Thick solid yellow lines ($M = 10$) and thick dashed pink lines ($M = 1$) represent upper/lower boundaries for silicate planets assuming a hot start along the solidus. The phase space of $M = 1$ is contained within the $M = 10$ phase space. Where the propensity trend is nonunique, i.e., in (a), (d), and (e), we illustrate how restrictions on initial state or composition help to better constrain results (see also Figure 2): thin dashed and dot-dashed (yellow for $M = 10$, pink for $M = 1$) lines represent in relation to initially hot silicate planets the widening of either the upper or the lower boundaries when either the assumption on initial temperature or composition is released—if those new curves are close to identical (within ∼5%), we plot a thin solid line (i.e., panel (a)). If the release of assumptions does not affect the boundaries, then we do not plot additional curves. Positive (negative) values indicate that the increase in planetary property increases (decreases) the propensity of plate tectonics; a green line indicates neutral zero.

We obtain these results by assuming that undifferentiated planets are dynamically approximated as a combination of our coreless planet with an increased Fe enrichment in mantle minerals. In this case, we can combine our results on coreless planets, mineralogically bound mantle Fe, and plate yielding (see the two previous sections and Figure 3).

Complicating our undifferentiated planet assumption is that iron could remain as clumps or in partially differentiated layers at lower pressures. These clumps might act as a low-viscosity region next to higher-viscosity silicates. However, our current understanding of the rheology of composites, though still limited, indicates that the rheology of the strongest compound controls the effective rheology (Yamazaki & Karato 2001; Karato 2008; Stamenković et al. 2011). Therefore, the included iron clumps should not critically impact the effective rock viscosity—supporting our initial assumption for undifferentiated planets. This is a first step toward understanding the dynamics of undifferentiated planets. We still have a long way to go with experiments and theory before we can fully grasp the nature of these planets.

3.6. Hypothetical Carbon Planets and Plate Yielding

We find that the interior history of carbon planets, independent of thermodynamic scenario and uncertainties in material properties, is quite different from silicate planets owing to much slower rock creep and greater thermal conductivities (see Appendix C.3.2.4). We find that the greater reference viscosity could, independent of χ, possibly lead to a lack of vigorous (upper) mantle convection on carbon planets.

Altogether, for $\chi_{\rm high}$, carbon planets have much lower propensities of plate tectonics than silicate analogs; for $\chi_{\rm low}$, carbon super-Earths of intermediate planet mass (M = 3–5) could be promising targets for the occurrence of plate tectonics (see Figure 4).

We explain these conclusions in this section: (1) for silicate planets (including Mercury-structured and all χ) we find, during 13 Gyr, Rayleigh numbers well above 10^5 and upper mantle viscosities below $\sim 10^{20}$–10^{22} Pa s, as well as lithospheric thicknesses of similar size to Earth-like-structured planets (10–400 km during 13 Gyr, much smaller than the mantle thickness). These results suggest vigorous upper mantle convection and deformable plates for silicate planets (see Figure 5 for $M = 1$) based on the criterion ($\delta_u + \delta_c \sim D$) as an indicator of a potential lack or a low vigor of convection (see Grott et al. 2011; Stamenković et al. 2012).

(2) In contrast to silicate planets, carbon planets have ∼10 orders of magnitude larger reference viscosities, ∼1 order of magnitude larger thermal conductivities, and ∼1 order of magnitude smaller thermal expansivities. Owing to the larger reference viscosity, the planet interior heats up more than for silicate analogs, supported by the greater thermal conductivity, which allows more heat to be released from the core into the mantle. However, the greater thermal conductivity also boosts upper mantle cooling, which buffers this additional heating. Altogether, although the upper mantles of carbon planets run generally a few hundred K hotter than their silicate analogs, upper mantle viscosities remain up to five orders of magnitude

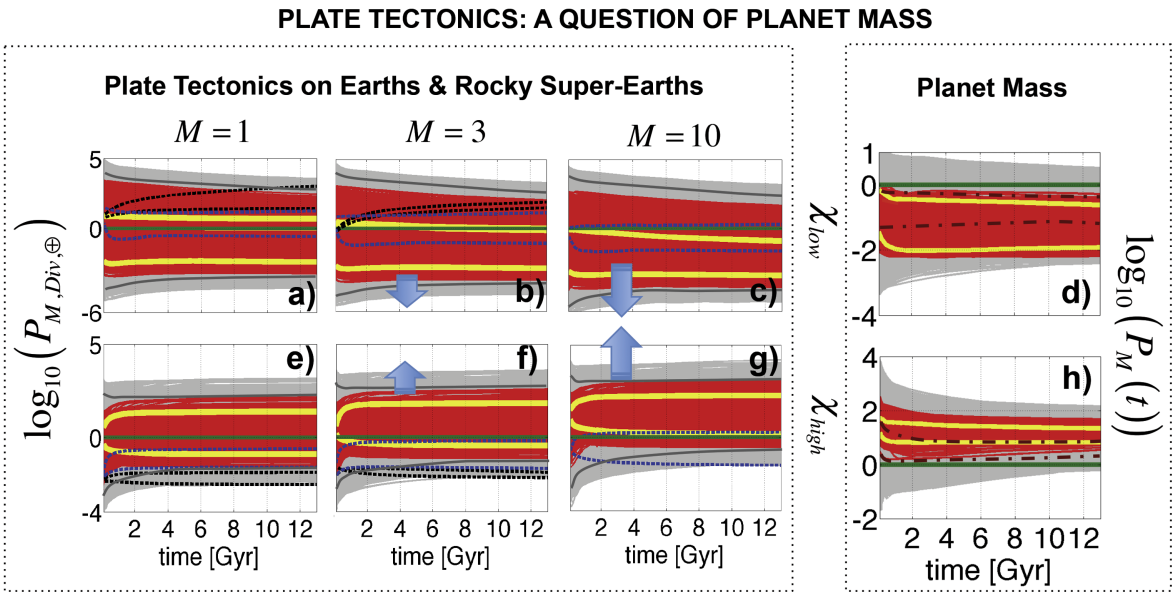

Figure 4. Plate tectonics on rocky super-Earths. For (d) and (h), we show plate tectonics propensity values for an increase of planet mass from $M = 1$ to $M = 10$ (and to $M = 3$ in brown). The gray envelope assumes the full range of planet parameters specified in Appendix C.3 and that the initial conditions of the $M = 1$, 10 planets could be anywhere between the "cool" and the "hot" start scenarios (so modeling sub-solidus convection for planets that start adiabatically or molten). The red envelope restricts the initial state of these $M = 1$, 10 planets to only "hot". Within the solid yellow boundaries are the propensities for an increased planet mass for silicate $M = 1$, 10 planets forming "hot" (most likely planet condition). The brown dot-dashed boundaries equal the red phase space for a planet mass change from $M = 1$ to $M = 3$ instead. For (a)–(c) and (e)–(g), we compare rocky super-Earths with our Earth model. The light gray shaded zone assumes the full range of planet parameters specified in Appendix C.3 with some restrictions (see note below). In comparison to the light gray area, we assume an Earth-like friction coefficient for the solid dark gray boundaries. The red envelope restricts the dark gray boundary space for planets forming molten. The solid yellow boundaries represent the propensity results for silicate planets forming molten with Earth-like friction coefficients in relation to Earth. Above these results, we plot the results for initially "hot" carbon planets: blue (black) dashed boundaries limit the propensity phase space of carbon planets where vigorous upper mantle convection and plate failure seem feasible (questionable) based on Section 3.6. Note the following: to reduce computation time (a)–(c) and (e)–(g) use a smaller set of parameters than those specified in Appendix C.3, but this does not alter the qualitative results (in particular the reference viscosity is varied by maximally five orders of magnitude, the activation energy is varied between 180–420 kJ mol^{-1}, and the thermal conductivity, expansivity, and capacity are varied by a factor of two in relation to reference values from Table 1).

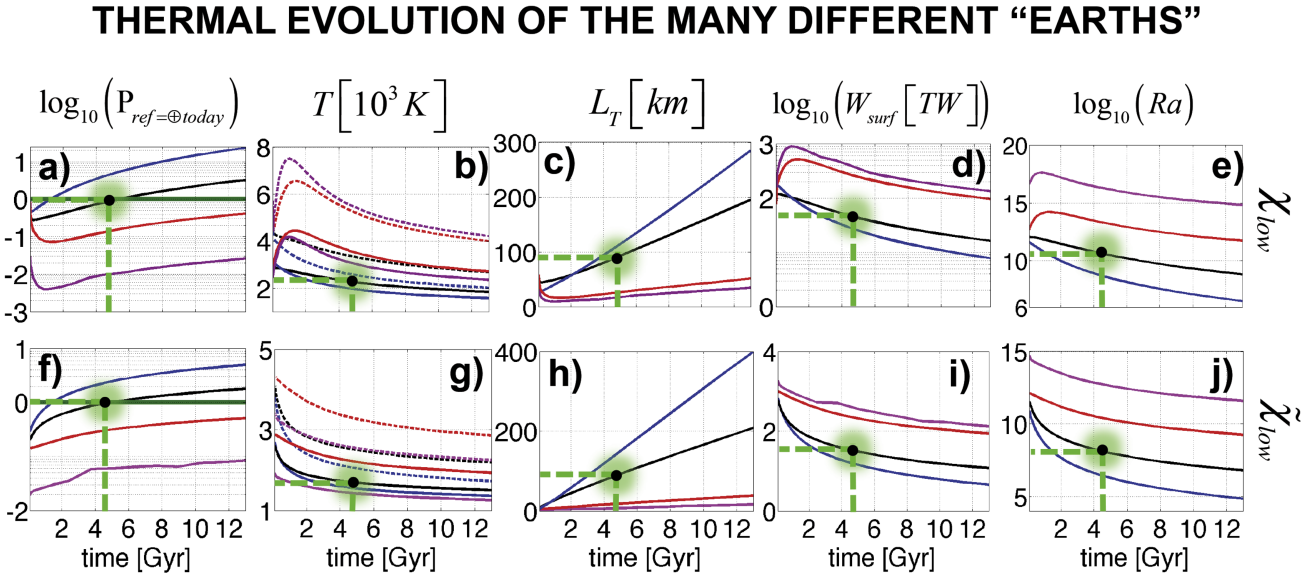

Figure 5. Evolution of interior properties for four Earth-mass planets starting "hot" in maintenance mode for our classic (β, γ) parameters used to illustrate $\chi_{\rm low}$ systems ($\chi_{\rm low}$), as well values of (β, γ) within $\chi_{\rm low}$ suggested by Stamenković & Breuer (2014) to better represent the evolution of a planet in active plate tectonics mode ($\chi_{\rm low}$ with ($\beta = 0.3$, $\gamma = 0.4\overline{3}$, F)), which we refer to as $\tilde{\chi}_{\rm low}$. (Black), reference Earth model; (Red, $Q = 10Q_{\oplus}$), like Earth but radiogenically enriched; (purple, $Q = 10Q_{\oplus}$, $f_c = 0$, $\eta_{\rm ref} = 10^{18}$ Pa s, $E^* = 255$ kJ mol^{-1}), like Earth but radiogenically enriched, no core, and Fe-enriched mantle; and finally (in blue) the "ideal" (within our parameter space) planet maximizing the propensity of plate tectonics, like Earth but depleted in radiogenic heat sources and Mercury-structure ($Q = 0.1Q_{\oplus}$, $f_c = 0.65$). The propensity of plate tectonics in comparison to our Earth model's value for today at 4.5 Gyr is $P_{\rm ref=\oplus today}(M, t) = X(M, t)[X(\oplus, t = 4.5\ {\rm Gyr})]^{-1}$; T stands for upper mantle temperature (solid) and CMB temperature (dashed); L_T is the thickness of the thermal lithosphere. $W_{\rm surf}$ is the surface power emission. Ra is the Rayleigh number. Results suggest vigorous mantle convection for at least 13 Gyr. In light green, we highlight the value at 4.5 Gyr for our Earth model.

greater at all times in relation to silicate analogs. Similar to the findings of Stamenković et al. (2012) for lower mantle dynamics of rocky super-Earths, the Tozer effect (Tozer 1967) is not fast enough to regulate the viscosity for too large viscosities.

(3) These large interior viscosities lead for carbon planets, independent of the thermodynamic scenario, to Rayleigh numbers significantly below 10^4 (often far below ∼100–1000 after a few Gyr), and for low heat sources and smaller Earth-sized planets the thermal boundary layers (especially the upper) become quickly large ($\delta_u + \delta_c \sim D$) at early times (a few Gyr). This suggests that (especially upper) mantle convection might not occur or be less effective (see similar argumentation for Mercury, e.g., Grott et al. 2011). However, without upper mantle convection, plate tectonics does not operate. We illustrate the possible lack of convection by plotting the propensity evolution boundaries for carbon planets in relation to Earth and highlight the zones where convection becomes questionable based on a boundary layer criterion ($\delta_u + \delta_c \sim D$) (in Figures 4(a)–(c), (e)–(g), black dashed boundaries). Note that within these black dashed boundaries Ra numbers are also far below 10^4 (∼100–1000 after a few Gyr).

(4) For $\chi_{\rm high}$, the possible lack of (upper) mantle convection and smaller propensities of plate tectonics in relation to silicate analogs or Earth ($P(t)$ is up to three orders of magnitude smaller; see Figures 4(e)–(g)) make plate tectonics on carbon planets for $\chi_{\rm high}$ less likely than on silicate analogs or Earth at all times.

(5) For $\chi_{\rm low}$, plate tectonics problems caused by a possible lack of vigorous mantle convection mix with larger propensities of plate tectonics for carbon planets in relation to silicate analogs owing to greater interior viscosities for carbon planets (propensity up to two orders of magnitude larger; Figures 4(a)–(c)). For carbon planets of intermediate mass $M = 3$–5, vigorous mantle convection seems feasible and propensities can be larger than Earth's values—making those intermediate-mass carbon planets possible candidates for plate tectonics to occur (the zone within blue dashed lines in Figure 4(b) has selected carbon planets with $log_{10}P_{M,\ Div}, \oplus > 0$).

3.7. Rocky Super-Earths and Plate Yielding

The question "How does planet mass impact the propensity of plate tectonics?" only has a unique answer if we know the initial thermal conditions of rocky planets (compare gray and red zones in Figures 4(d) and (h)). For all planets forming "hot" along the mantle solidus (the same if all planets start in the "cool" adiabatic scenario), we find that for the $\chi_{\rm low}$ model, plate tectonics is less likely when the planet mass increases independent of a planet's composition and its structure. For $\chi_{\rm high}$, we find that plate tectonics is more likely when the planet mass increases independently of a planet's composition and its structure.

Asking how increasing planet mass impacts the propensity of plate tectonics for a specific planet with given composition and structure does not answer whether rocky super-Earths are more or less likely to have plate tectonics in comparison to Earth: to answer such a question, we must check in Figures 4 (a)–(c) and (e)–(g) whether a rocky super-Earth of arbitrary composition and structure has a larger or smaller propensity of plate tectonics values than Earth at all times. We find that without knowledge of initial interior temperatures and planet composition or structure, plate tectonics could be less or more likely on rocky super-Earths than on Earth, independent of χ owing to a different composition or structure (in Figures 4 (a)–(c) and (e)–(g), the gray zone is the propensity phase space in relation to Earth without any restrictions on planet composition, lithospheric friction coefficients, and initial state). However, depending on χ, there is a clear trend for shifting the propensity values for more massive planets in relation to Earth upward ($\chi_{\rm high}$) or downward ($\chi_{\rm low}$) in propensity space (see arrows in Figures 4(a)–(c) and (e)–(g)).

Within our large pool of varied planet properties (C.3), we can only identify silicate and carbon planets (C.3.2.4). Looking at this group of planets, we see that for $\chi_{\rm high}$, it is especially initially "hot" silicate super-Earths that have the largest propensity of plate tectonics values amongst all studied planets (the space between the thick yellow lines in Figure 4(e)–(g) has some of the largest propensity values). On the contrary, for $\chi_{\rm low}$, the only super-Earths that have propensity values larger than the Earth and seem to have vigorous convection are certain selected carbon super-Earths of intermediate planet mass ($M \sim 3-5$, see Figure 4(a)–(c)). In Section 4.2.3 we discuss super-Earths with compositions between silicate and carbon planets that might also be interesting targets for the occurrence of plate tectonics.

4. DISCUSSION

The intrinsically probabilistic nature of any description of plate tectonics occurrence limits what we can say about an individual planet. Progress can still be made by statistically linking geophysics with a set of astrophysical observables. We created a framework as a function of two thermodynamic models, which describe how planet mass, composition, structure, initial conditions, and time impact plate yielding, a fundamental requirement for plate tectonics.

Our model is an evolving framework: in time, we can refine it by accounting for subduction efficiencies, a more complex rheology, grain size, or memory. Although such extensions of our model seem interesting, we should also emphasize that even in its current form (1) our model is in good agreement with observed trends from numerical 2D and 3D plate tectonics experiments, and (2) it provides reasonable explanations for many dynamic aspects of plate tectonics (or lack thereof) as seen in our solar system and on Earth. Also, we note that the often-inferred mismatch between experimentally determined lithospheric strength and convective stresses can be significantly reduced via stress amplification induced by sublithospheric channels (e.g., Richards et al. 2001; Höink & Lenardic 2010; Stamenković et al. 2016).

Our "qualitative" probabilistic approach toward plate tectonics is related to Lenardic & Crowley (2012). Their study of an intrinsic bi-stability of the tectonic mode is a mandatory addition to the current discussion of how "predictable" the tectonic mode is. Based on their findings, it would be interesting to check whether bi-stability results from studying initiation and maintenance separately or from an intrinsic bifurcation along any thermal evolution path.

4.1. The Occurrence of Plate Tectonics across the Galaxy

In this section, we focus on the implications for the occurrence of plate tectonics across the Galaxy for $\chi_{\rm low}$ and silicate and carbon planets. We additionally discuss the implications if for smaller planets and maintenance $\chi_{\rm high}$ was valid instead, as suggested by Stamenković & Breuer (2014). In Section 4.2.3 we discuss other good candidates for the occurance of plate tectonics outside of the family of carbon and silicate planets.

4.1.1. Toward the Ideal Candidate for Plate Tectonics

Based on our current understanding and for the range of varied planet conditions for silicate and carbon planets, the ideal candidate that maximizes the propensity of plate tectonics would be an Earth-mass silicate super-Mercury planet with small concentration of radiogenic heat sources ($\sim 0.1 Q_{\oplus}$) and as little iron as possible within its mantle. As differentiation is highly likely to occur for Earth-sized planets (Breuer & Moore 2015), characteristics of such planets would be a larger average rocky body density of $\sim 7000\,{\rm kg\,m^{-3}}$ ($\sim$30% denser than the Earth-like analog)—which could be confirmed with simultaneous radial velocity and transit measurements. The evolution of such a planet is illustrated in Figure 5 in comparison to our Earth model. Moreover, some essential information contained within Figure 5(a) is that the propensity of maintaining plate tectonics increases with the time as the planet cools, and that the Rayleigh number and thermal boundary layer thicknesses are respectively above 10^5 or much smaller than the mantle depth even after 13 billion years of planet evolution, indicating still vigorous mantle convection. This means that Earth and our ideal candidate might enjoy the benefit of plate tectonics for well over 13 Gyr. Ultimately, however, there will be a later point in time when the convective vigor will become subcritical and convection and plate tectonics will cease.

Please note that some selected carbon planets of intermediate planet mass ($M \sim 3-5$) might also be interesting candidates for the occurrence of plate tectonics–but their probability is difficult to assess.

4.1.2. Hotter Is Not Always Better—a Common Misconception

Radiogenic heat sources are needed to drive mantle convection and plate tectonics. However, it is a common misconception that more heat sources always lead to an increased vigor of plate tectonics. For $\chi_{\rm low}$, the propensity of plate tectonics declines when interior heat increases. This is because convective stresses scale not only with convective velocity but also with mantle viscosity. Therefore, convective stresses strongly decrease as a result of decreasing viscosities for $\chi_{\rm low}$ (in agreement with Stein et al. 2011, 2013; Jellinek & Jackson 2015).

A small heat source concentration, however, does not mean no heat sources. We obviously need enough heat sources to allow vigorous convection. For our studied values of 0.1–10 times Earth's radiogenic heat concentration, a natural variation suggested by ISM evolution models, our $\chi_{\rm low}$ models result in convection throughout 13 Gyr for silicate planets ($\delta_u + \delta_c \ll D$). Although a critical concentration of radiogenic heat sources is needed for plate tectonics to operate, beyond this threshold more does not increase the propensity of plate tectonics.

4.1.3. A Late Start for Plate Tectonics? In the Outer Galactic Disk Only?

From an astrophysical viewpoint, we want to know where we could find planets that support the occurrence of plate tectonics. This sentiment remains despite this paper's emphasis on a probabilistic assessment of what planet properties are most favorable for plate tectonics.

From a probabilistic perspective, and assuming $\chi_{\rm low}$ and lid failure analysis, we assert that the best planet candidates for plate tectonics are those orbiting young, high-metallicity stars found in the outer disk of the Milky Way. This leads to the speculation that the early universe might have been too hot, too rich in oxygen, but too poor in iron to form planets that could have supported plate tectonics, and that planets supporting plate tectonics might have started forming increasingly 8 Gyr ago in the outer disk.

The conclusion above is based on the following argumentation: (1) from a statistical order-of-magnitude perspective, host stars and their orbiting rocky planets reflect to some degree (the chemical host star evolution, type, and age must be accounted for) the average metal ratios of the ISM they formed in (e.g., Bond et al. 2010). We cannot make a one-to-one correlation between a host star's metal abundances and its rocky planets. All we can say is that planets orbiting stars, which formed from an ISM depleted in metallic element X (e.g., radiogenic heat sources), are more likely to be depleted in that very same metallic element X. Knowing how chemical abundances have evolved in the ISM in time, therefore, allows us to make, from a probabilistic perspective, order-of-magnitude estimates on the evolution of rocky planets with time after the big bang and to correlate average planet properties to a planet's host star metallicity and age. (2) For the evolution of the ISM, we are specifically interested in how the concentration of radiogenic heat sources (such as thorium, potassium, and uranium), silicon, and oxygen as compared to iron evolved in time and location. We use ISM evolution models based on the concept of primordial content being enriched over time: the ISM is composed of primordial elements such as H, He, and Li and is being continuously enriched in time from the remnants of dead stars in heavier elements from primary (e.g., local supernova) and secondary sources (e.g., stellar neighborhood). The general conclusion in current literature is that with time after the big bang, Si/Fe, O/Fe, and Q/Fe concentrations decrease with time (e.g., Clayton 1988; Timmes. et al. 1995; Gonzalez & Brownlee 2001; Ramirez et al. 2013), and that there is no clear correlation between the formation probability and the mass distribution of a rocky planet with host-star metallicity (e.g., Buchhave et al. 2012, 2014). (3) Therefore, from a probabilistic perspective, the early universe was more likely to form rocky planets with small cores, large initial amounts of radiogenic heat sources, and a more oxidized mantle. Also, the oxidized mantle adds a greater capacity to keep iron within the rocky mantle and increases the chances of a smaller core. (4) As shown by Bergemann et al. (2014), there is evidence that younger evolved stars with larger metallicities are generally found in the outer disk and that stars formed more than 8 Gyr ago have steeply decreasing metallicities. (5) Points 1–3 in combination with our propensity of plate tectonics results from

Section 3 lead to the conclusions at the beginning of this section.

The findings presented above are speculative, and a definite answer demands more work, especially in understanding how the Mg/Fe ratio changing in time and space might complicate our results by modulating mantle viscosity and core size. Also, this result does not account for the potential likelihood of plate tectonics on intermediate planet mass carbon or carbon-rich (see Section 4.2.3) super-Earths, or how O/C ratios evolved in time. However, the results presented here give a first glimpse into the methodology needed to understand the distribution of plate tectonics planets in time and space in our Galaxy.

4.2. Magnetic Fields, Exogeodynamics, and the Way Forward

4.2.1. Magnetic Fields

Various papers have studied the propensity of rocky exoplanets to generate magnetic dynamos (e.g., Gaidos et al. 2010; Driscoll & Olson 2011; Tachinami et al. 2011). However, similar to the here-illustrated case of plate tectonics, we should address any questions regarding dynamo generation on rocky exoplanets while aiming to incorporate as many uncertainties as we can. Those uncertainties increase for more massive planets. For dynamo generation critical uncertainties are the pressure dependence of mantle rheology (results differ by about 15 orders of magnitude for the same temperatures; see, e.g., Karato 2011; Stamenković et al. 2011; Tackley et al. 2013), the melting temperatures of mantle rock and iron (results differ by about 10,000 K for the melting temperature of pure MgO at 1 TPa; see, e.g., Valencia et al. 2006; Stamenković et al. 2011), and initial conditions. These uncertainties can lead to a complete thermal insulation with no thermal or compositional dynamo generation for rocky super-Earths (i.e., Stamenković et al. 2012) or to high heat fluxes, which easily enable thermal dynamo generation (i.e., Driscoll & Olson 2011). Therefore, currently it is especially difficult to estimate the ability of rocky super-Earths to generate magnetic fields. Small close-by rocky exoplanets, as found in the Trappist-1 system, might help to reduce these uncertainties (Gillon et al., 2016).

4.2.2. Exogeodynamics and the Way Forward

We still have not fully understood how plate tectonics operates on Earth. A fundamental uncertainty is represented in our model with the two different thermodynamic scenarios. It might, therefore, seem questionable why we try to explore plate tectonics on other bodies in our solar system and on exoplanets. The main benefit from studying plate tectonics on alien worlds lies in leaving the comfort zone of our assumptions made for Earth—assumptions that have maybe been taken for granted for too long (see Stamenković et al. 2016). By doing so, we can rediscover the processes causing plate tectonics from a more fundamental and universal perspective. We now need to make advances in understanding which stress type as a function of time drives plate failure and subduction. We have made first steps toward this goal (Stamenković et al. 2016), but much more work is needed with time-dependent models with more realistic boundary conditions and model parameters. Especially interesting is to study whether there is a transition from $\chi_{\rm low}$ to $\chi_{\rm high}$ when transitioning from initiation to maintenance scenarios or from small to large Rayleigh numbers.

Although the future of exogeodynamics is promising, one limitation will forever remain: large degeneracies will prevail when trying to estimate the interior composition of a planet from bulk planet and host-star observations. Even for the ideal case of knowing exactly what the planet's composition and structure is, we will never know the planet's initial conditions and history, which can significantly impact the tectonic mode of a rocky planet. So even in the best case, we will only be capable of assessing the probability of a planet to have plate tectonics. But such a probability in combination with a statistical "planet host star connection" may allow us to distinguish zones in the Milky Way with greater and smaller chances of finding planets with plate tectonics, and therefore help us to choose which planet candidates are better suited for spectroscopic follow-up missions when looking for life or searching for Earth 2.0, in our solar neighborhood or beyond.

Once more detailed maps of rocky exoplanets become feasible, other possibilities to estimate whether a planet has active plate tectonics or not might emerge by better understanding how plate tectonics impacts climate and especially the cloud distribution in relation to continents and oceans. Plate tectonics is responsible on Earth for continental uplift, which drives mountain formation, and cloud formation from coast to mountain peaks—leaving a fingerprint on cloud versus continent distribution. Therefore, clouds, which currently limit spectroscopic observation of exoplanet atmospheres, might actually one day help to determine whether there is plate tectonics on an exoplanet or not.

4.2.3. Worlds between Silicate and Carbon

We have focused on silicate and carbon planets but tested a much wider parameter space in thermal and transport properties to see whether our results in Figures 2, 3, 4(d), and 4(h) are robust for a wide and yet uncertain spectrum of planets. However, Figures 4(a)–(c) show that for $\chi_{\rm low}$, super-Earths with vigorous mantle convection may exist where propensity values are greater than those for our ideal silicate case from Section 4.1.1 or for intermediate mass carbon planets. These are those planets with positive propensity values above the top solid yellow line in Figures 4(a)–(c) that have vigorous mantle convection. Such planets have thermal and transport properties in between the values for silicate and carbon planets. They could represent carbon-rich silicate planets but our knowledge on the rheology of composites is still too modest to allow us to draw any conclusions. Nonetheless, this illustrates the need to better explore the realm of carbon-rich rock, as such potentially "carbon-rich" silicate worlds might be, in the case of $\chi_{\rm low}$, the best super-Earth candidates for plate tectonics to occur.

5. CONCLUSIONS—UNCERTAINTY REMAINS BUT PROCESSES AND PREDICTABILITY EMERGE

We have explored a qualitatively probabilistic framework of how the propensity of plate tectonics is affected by planet conditions—from planet mass, structure, and composition to initial conditions. We then applied this framework to discuss where in our Galaxy planets exist that are most likely to support the occurrence of plate tectonics.

We have used a 1D thermal evolution and plate yielding model to study plate tectonics. The model is simple, yet has good agreement with 2D and 3D numerical models (see Stamenković et al. 2012, 2016; Stamenković & Breuer 2014).

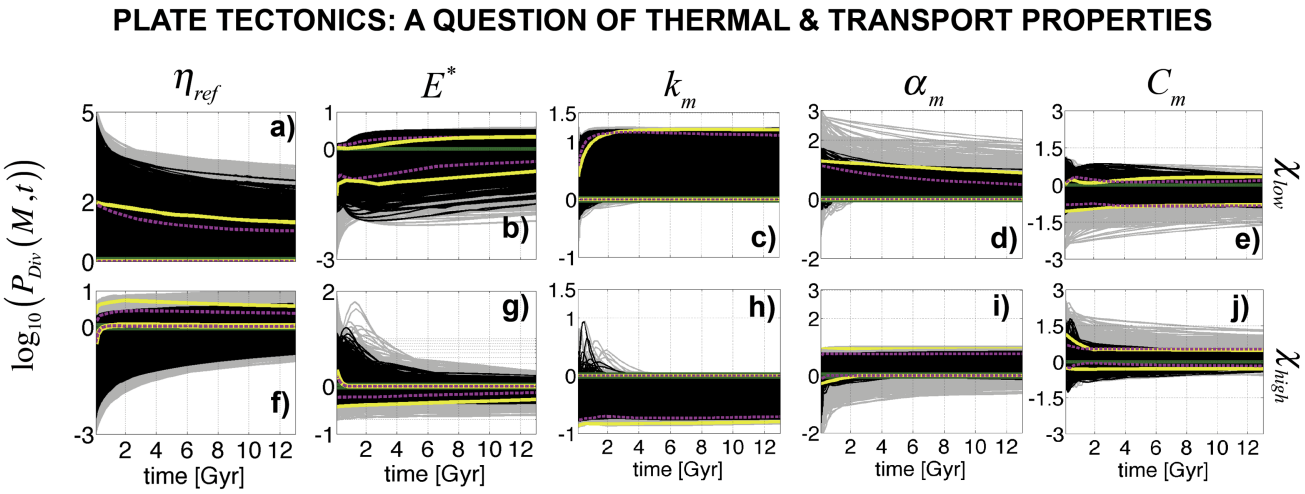

Figure 6. Impact of varied mantle thermal and transport properties on the propensity of plate tectonics for $\chi_{\rm low}$ and $\chi_{\rm high}$. For nomenclature see Figure 3. We plot the decimal logarithm of the propensity of plate tectonics during 13 Gyr for an increase of mantle rock reference viscosity $\eta_{\rm ref}$ ((a), (f), 10^{-5} to 10^{5} times the standard Earth value) and mantle rock activation energy E^* ((b), (g), ± 120 kJ mol^{-1} from the standard Earth value); the thermal conductivity k_m ((c), (h)), the thermal expansivity α_m ((d), (i)), and the specific heat C_m ((e), (j)) are 0.5–2 times the Earth reference value (see Table 1).

In the future we will be extending the sophistication of our 1D model if shown to be necessary.

Our main finding is that many factors impact plate tectonics, some as much as or more than planet mass, typically assumed to be the dominant factor. Which properties or conditions increase the propensity of plate tectonics generally depends on which thermodynamic scenario, $\chi_{\rm low}$ or $\chi_{\rm high}$, best represents planetary interiors. The χ regime describes how plate tectonics reacts to a change of heat. The $\chi_{\rm low}$ scenario leads to plate tectonics being less likely for a hotter interior, and $\chi_{\rm high}$ leads to the opposite behavior. Those two thermodynamic scenarios are directly related to questions such as which stress type (surface normal or basal shear) drives plate yielding, and how time dependence of stresses, realistic boundary conditions, and viscosities impact planet evolution (i.e., Stamenković et al. 2016). We do not yet have enough information to know which thermodynamic model is more realistic. However, in Stamenković & Breuer (2014) and Stamenković et al. (2016), we find suggestive evidence supporting $\chi_{\rm low}$.

Our general framework gives predictions based on the thermodynamic scenario and might change in the future when our understanding of the correct thermodynamic scenario evolves. The results that are robust and independent of the thermodynamic scenario are as follows:

1. Plate tectonics on rocky super-Earths can be more or less likely than on Earth, depending on planet composition, structure, initial state, and history.
2. Iron-rich mantle rock reduces the propensity of plate tectonics occurring on silicate planets like Earth if those planets formed "hot" (along or above mantle solidus).
3. Carbon planets are generally not ideal candidates for plate tectonics (with some exceptions for $\chi_{\rm low}$; see below) because of the slower creep rates and higher thermal conductivity for SiC in comparison to silicate planets.

All other conclusions strongly depend on our choice of a thermodynamic framework for plate tectonics. For $\chi_{\rm low}$, where the propensity of plate tectonics decreases with increasing interior heat, and assuming that all planets form "hot" (initial interior temperatures along or above mantle solidus), we find, within our range of varied planet conditions, that the planets with the greatest propensity of plate tectonics are silicate rocky planets of $\sim$1 $M_\oplus$ with large metallic cores (average density $\sim$5500–7000 kg m^{-3}) with minimal mantle concentrations of iron (as little as 0% is preferred) and radiogenic isotopes at formation (up to $\sim$10 times less than Earth's initial abundance; less heat sources do not mean no heat sources). Such planets are suggested to be common around young stars in the outer disk of the Milky Way. Rocky super-Earths, undifferentiated planets, and still hypothetical carbon planets have higher chances of being stagnant lid planets, although for $\chi_{\rm low}$, carbon super-Earths of intermediate planet mass ($M \sim 3-5$) could be favorable for the occurrence of plate tectonics, as well as super-Earths with compositions between silicate and carbon planets, which have yet to be explored.

One major conclusion remains in spite of all uncertainties: to better understand the deep interior of exoplanets, we should explore the thermodynamic basics of thermal evolution and plate tectonics and study plate tectonics from a probabilistic perspective. This will allow us to bridge Earth science with exoplanet research in a way that is constructive for both disciplines.

V.S. thanks the Simons Foundation for kindly supporting this work through a "Simons Collaboration on the Origins of Life" fellowship (338555, VS), Adrian Lenardic, Tobias Höink, and Doris Brever for insightful discussions, an anonymous reviewer for comments, and Steinn Sigurdson for his editorial work.

APPENDIX A
THERMAL AND TRANSPORT PROPERTIES AND PLATE YIELDING

We show how plate yielding and hence the propensity of plate tectonics depend on changes in thermal and transport properties, such as activation energy and reference viscosity, the thermal expansivity and conductivity, and the heat capacity of mantle rock. This helps in understanding how a change in planet composition affects the propensity of plate tectonics, which has been shown in the main body of the paper (Figures 2–4).

A.1. Viscosity—the Major Game Changer

The linear mantle rock rheology depends in our model solely on reference viscosity and activation energy. The effect of activation energy on the propensity of plate tectonics depends on planet composition and structure; the effects of reference viscosity on the propensity of plate tectonics depend strongly on the thermodynamic scenario (Figure 6).

For $\chi_{\rm low}$, increasing reference viscosity leads to an increasing plate tectonics propensity owing to the viscosity control for $\chi_{\rm low}$ systems—this increase is, however, damped by the fact that an increased reference viscosity also increases interior temperature, which, on the other hand, reduces propensities (however, this damping is small as temperature changes in $\chi_{\rm low}$ systems are rather slow; see Stamenković & Breuer 2014).

For $\chi_{\rm high}$, plate tectonics is instead controlled by convective velocities. Because larger viscosities reduce convective velocities, plate tectonics propensities are generally reduced when $\eta_{\rm ref}$ increases. This decrease is, however, strongly modulated by the fast increasing interior temperatures, which especially for the low-viscosity systems (silicate planets) can even change this trend and increase the propensity of plate tectonics.

Increasing activation energies initially decrease viscosities for the same initial temperatures ($\eta \propto \exp(-E^*(T - T_{\rm ref})T^{-1}T_{\rm ref}^{-1})$) and hence impact plate tectonics to a first order early on in time just like decreasing $\eta_{\rm ref}$. However, larger E^* also allow the planet to cool faster than when just $\eta_{\rm ref}$ is reduced (viscosity adjusts faster owing to the exponential feedback between E^* and viscosity [instead of the linear feedback for $\eta_{\rm ref}$] in $\eta \propto \eta_{\rm ref}\exp(-E^*(T - T_{\rm ref})T^{-1}T_{\rm ref}^{-1})$—this not only dampens the early first-order effect, contrary to increasing $\eta_{\rm ref}$, but can also reverse it.

A.2. Thermal Properties

The variation of average thermal properties due to bulk composition changes impacts the propensity of plate tectonics significantly (see Figure 6).

In summary, (1) effects of the thermal expansivity $\alpha_{\rm m}$ and heat capacity $C_{\rm m}$ are much stronger for more massive planets—owing to the adiabatic temperature increase depending on $\alpha_{\rm m}$ and C_m and directly scaling with mantle depth; (2) for $\chi_{\rm low}$ systems, increasing thermal expansivities have a similar effect to increasing thermal conductivities on the propensity of plate tectonics; (3) increasing thermal conductivities induce greater planetary cooling except early in a planet's history, where they also increase the core heat flux, which heats up the upper mantle at early times up to ~2 Gyr.

The summary above is based on the following arguments: heat capacity and thermal expansivity are varied independently from each other. However, in reality they are connected via thermodynamic relations (e.g., Stamenković et al. 2011). The thermal expansivity of rock is more sensitive to rock composition than the heat capacity, which is of a smaller importance to planetary evolution (i.e., Stamenković et al. 2011). Increasing thermal expansivities and heat capacities have generally contrary effects on the propensity of plate tectonics. This is due to the fact that the adiabatic gradient, which strongly affects interior temperatures, is proportional to $\partial T_{\rm adia}/\partial P \propto (\alpha_m/C_m)$, where P is pressure. Bearing in mind that the Rayleigh number scales with $\mathrm{Ra} \propto (\alpha_m C_m)$ and that the static factors for the maintainance of plate tectonics scale like $X \propto {\alpha_m}^{\chi}{C_m}^{\chi-1}$ (see Equation 16) suffices to explain that increasing thermal expansivities cool the upper mantle (by stabilizing a hotter core via larger adiabatic gradients, hence reducing the core heat flux, and by additionally cooling the upper mantle through greater Ra numbers). These effects combined enlarge the propensity of plate tectonics for $\chi_{\rm low}$ when α_m increases. For $\chi_{\rm high}$, we obtain a mixed behavior of the propensity of plate tectonics when α_m changes, as cooling effects, which tend to decrease the propensity of plate tectonics, blend with static contributions that increase the propensity of plate tectonics. Owing to the adiabatic gradient being $\partial T_{\rm adia}/\partial P \propto (\alpha_m/C_m)$, an increasing heat capacity impacts, to a first order, plate tectonics contrary to increasing α_m. However, this contrary behavior between α_m and C_m is modulated by $\mathrm{Ra} \propto (\alpha_m C_m)$, explaining why an increase in heat capacity does not have a uniquely positive or negative effect on the propensity of plate tectonics.

APPENDIX B
MELT GENERATION AND PRESSURE-DEPENDENT VISCOSITY

We discuss how an inclusion of melt generation and extraction and pressure-dependent viscosity impact the results presented in the main body of the paper.

B.1. Implications of Melt—"Damping" but Same Trends

We use the melt generation and extraction model, as well as the mantle solidus specified in Stamenković & Breuer (2014), where excess melt is removed to the surface by volcanism wherever the interior temperature exceeds the solidus of mantle rock. This overestimates the impact of melt. We find that our results on how the propensity of plate tectonics depends on initial conditions, mass, structure, radiogenic heat sources, and iron remain similar after including melt within our model (accounting for melting temperature changes for different activation energies based on the homologous temperature approach; see Stamenković et al. 2011; Karato 2008), although the observed effects are damped. This damping is expected as compositional and structural changes can be related to thermal changes and as an inclusion of melt dampens thermal differences between various initial conditions (Stamenković & Breuer 2014).

B.2. Implications of Pressure Dependence—Initial Conditions Matter Even More and Massive Planets Become More Uncertain

The major uncertainty when considering interior properties and the thermal evolution of planets (especially of rocky super-Earths) is the pressure dependence of mantle viscosity (Karato 2011; Stamenković et al. 2011, 2012; Tackley et al. 2013).

It seems reasonable to assume that activation volumes are significantly large to strongly affect the interior heat transport especially in super-Earths, which is now supported by shock-wave melting experiments on MgO (McWilliams et al. 2012).

Nonetheless, there are still uncertainties associated with such melting experiments and also with ab initio studies (they lack the ability to quantify the extrinsic vacancy concentration). We must wait for future diamond anvil cell experiments to provide

better answers or start using Earth's history and current interior constraints to refine our understanding of Earth's rheology.

We cannot yet use our plate tectonics model to predict strong pressure-dependent viscosity effects on massive rocky planets. This is because the scaling used for studying plate tectonics fails when sluggish lower mantle convection occurs, which is possible on massive rocky super-Earths for large activation volumes (Stamenković et al. 2012). However, we can study effects of large activation volumes on plate tectonics on an Earth-sized planet, where we always found vigorous full mantle convection with 2D spherical convection models (Stamenković et al. 2012). When we model Earth with activation volumes from Stamenković et al. (2011), we find our general conclusions on how planet diversity shapes plate tectonics unchanged for an Earth-sized planet. This is not surprising as we beforehand intentionally included high $\eta_{\rm ref}$ and E^* runs—which resemble pressure-dependent viscosities.

However, for massive planets, we can only speculate how $V^*_{\rm eff} > 0$ impacts plate tectonics: we can refer to our previous result that the strong pressure dependence of the viscosity leads to initial conditions being more important especially for rocky super-Earths (Stamenković et al. 2012). This leaves super-Earths that start along the mantle solidus hot for much longer than for $V^*_{\rm eff} = 0$ with a lower mantle that can be partially sluggish (see Stamenković et al. 2012).

Our previous results are based on a diverse variety of planet structures and initial conditions, and therefore we do not expect that compositional and structural effects for $V^*_{\rm eff} > 0$ will significantly vary from $V^*_{\rm eff} = 0$ even for super-Earths.

However, we expect that our conclusions on how the propensity of plate tectonics changes with increasing planet mass will differ, as an increase in planet mass now correlates to an additional increase in interior heat and a reduced stress scale. As we argue in Stamenković & Breuer (2014), this does seem to still support our finding that plate tectonics less likely occurs on rocky super-Earths based on a failure criterion and $\chi_{\rm low}$. However, how viscosity changes with pressure is, after constraining χ, the most crucial current limitation to understanding massive rocky planets.

APPENDIX C
DETAILS ON THE GENERAL FRAMEWORK

We present equations for maintenance and refer to Stamenković et al. (2012) and Stamenković & Breuer (2014) for stagnant lid scalings.

C.1. Thermal Evolution Model

For the maintenance scenario, δ_u equals the thermal lithosphere L_T, and the following equations, in combination with the energy conservation within the planet (e.g., Stamenković et al. 2012), allow modeling the thermal history of a planet's interior (see Figure 1):

$$\delta_u = D({\rm Ra}/{\rm Ra}_{\rm crit})^{-\beta}, \tag{6}$$

$$\delta_c = ((\eta_c \kappa_m 0.28 Ra^{0.21})/(\alpha_m \rho_m g \Delta T_c))^{\frac{1}{3}}, \tag{7}$$

$${\rm Ra} = \alpha_m \rho_m g D^3 \Delta T/(\kappa_m \eta_m). \tag{8}$$

The thermal boundary layers scale as functions of the Rayleigh number Ra (standard definition of Rayleigh number for basally heated systems), which represents the convective vigor within the mantle, the thickness of the convecting mantle D, a constant critical Rayleigh number of ${\rm Ra}_{\rm crit} \sim 1000$, and the Nusselt–Rayleigh exponent $\beta \in [1/5, 1/3]$ depending on boundary conditions, mode of heating, Ra number regime, and lower–upper mantle interaction. Values of β much smaller than $1/5$ or negative values (Korenaga 2003) have not been confirmed by 2D/3D numerical experiments, and hence we did not explore them. The total temperature drop over (δ_u, δ_c), $\Delta T = \Delta T_u + \Delta T_c$, is used to compute the Rayleigh number and the mantle (core) heat fluxes $q_m = k_m \Delta T_u \delta_u^{-1}$ ($q_c = k_m \Delta T_c \delta_c^{-1}$). The surface gravity is g, α_m is the average mantle thermal expansivity, ρ_m is the average mantle density, k_m is the average mantle thermal conductivity, C_m is the average mantle heat capacity, and $\kappa_m = k_m C_m^{-1} \rho_m^{-1}$ is the average mantle thermal diffusivity. We use non-depth-dependent values for thermal properties, as we do not find significantly different plate tectonics results when accounting for their depth dependence (Stamenković & Breuer 2014).

To compute Rayleigh numbers, the mantle heat flux, and thus also the upper thermal boundary layer, the upper mantle viscosity $\eta_m = \eta(T_m)$, decreasing with temperature $T_m(t)$, is used. To better model strongly temperature-dependent systems, it has been shown that it is more appropriate to use an average viscosity within the lower thermal boundary layer $\eta_c \approx \eta(T_c - \Delta T_c/2)$ and a critical Rayleigh number being a function of the Rayleigh number (i.e., Deschamps & Sotin 2000). We have shown in Stamenković et al. (2012) and Stamenković & Breuer (2014), by running many simulations, that this specific choice of critical Rayleigh number and lower thermal boundary layer parameterization does not impact our findings, which are mainly controlled by the evolution of the upper mantle (hence by χ).

C.2. Plate Tectonics Model—a Dynamic Focus on Plate Failure

For our qualitative trend based approach, the relevant yield stress of the plate is assumed to be proportional to the pressure at the base of the thermal lithosphere (e.g., Byerlee 1968; Moresi & Solomatov 1998; O'Neill et al. 2007) and is

$$\tau_y \propto g \rho_{\rm up} C_{\rm fric} \delta_u \propto g C_{\rm fric} D {\rm Ra}^{-\beta}, \tag{9}$$

where $\rho_{\rm up} = \rho_{{\rm up},\oplus}$ is the average lithosphere density similar for all rocky planets (e.g., Sotin et al. 2007, and Section C.3), and $C_{\rm fric}$ is the friction coefficient of lithospheric rocks.

The scaling laws for the driving stress equaling the basal shear stress (τ_{zx}) or the normal stress (τ_{zz}) are based on the scaling laws for convective velocity v_c and the length of convective cells Λ (~plate length), which demand next to β two additional scaling parameters (γ, ε), with $\gamma \in [2/5, 2/3]$ and $\varepsilon \in [0, 1/6]$ as derived in many 2D/3D numerical models (see Stamenković & Breuer 2014 for a summary). R is the outward planet radial scalar:

$$v_c \propto \kappa_{up} D^{-1} (Ra Ra_{crit}^{-1})^{\gamma} \tag{10}$$

$$\tau_{zx} = \eta_m (\partial v_c/\partial R) \tilde{\propto} \eta_m D^{-1} v_c \propto \kappa_{up} \eta_m D^{-2} (Ra Ra_{crit}^{-1})^{\gamma} \tag{11}$$

$$\Lambda \propto D {\rm Ra}^{-\varepsilon}, \tag{12}$$

$$\tau_{zz} \tau_{zx}^{-1} = \Lambda \delta_u^{-1}. \tag{13}$$

With the scalings from Equations (6)–(13), the failure function X defined in Equation (2) can be computed for the F and S

model (X_F and X_S respectively) for maintenance:

$$X_F(M, t) = \tau_{zx}\tau_y^{-1} \propto \left(gD^2C_{fric}\right)^{-1}\kappa_{up}\eta_m Ra^{\gamma}\delta_u^{-1} \quad (14)$$

$$X_S(M, t) = \tau_{zz}\tau_y^{-1} = \tau_{zx}\tau_y^{-1}\Lambda\delta_u^{-1} = F\Lambda\delta_u^{-1} \propto \left(gDC_{fric}\right)^{-1}\kappa_{up}\eta_m Ra^{\gamma-\varepsilon}\delta_u^{-2} \quad (15)$$

These explicit failure functions can now be used to compute the propensity of plate tectonics for a variety of planets as defined in Section 2.

Both failure functions depend critically on the variable χ, as defined in Section 2.1.2. This dependence on χ can be seen for maintenance, where X as a function of χ is

$$X(M, t, T_0, comp., struct., \chi) \propto C_{fric}^{-1}g^{\chi-1}D^{3(\chi-1)} \times \kappa_{up}\left(\rho_m\alpha_m\kappa_m^{-1}\right)^{\chi}(\eta_m)^{1-\chi}(\Delta T)^{\chi} \quad (16)$$

The lithospheric thermal diffusivity is $\kappa_{\rm up} = k_m C_m^{-1}\rho_{\rm up}^{-1}$. Replacing $\rho_{\rm up}$ with ρ_m for all scalings (e.g., $\kappa_{\rm up}$, Equation (9)) does not affect our results, as the viscosity and thermal conductivity differences between planets mainly control the propensity of plate tectonics. Note that Equation (16) differs slightly from Equation (20) in Stamenković & Breuer (2014), where we did not account for compositional differences between planets.

C.3. Parameters and the Limits to Rocky Planet Diversity

We explain in the following how we vary planet structure, composition, and initial conditions, and where the parameter values for material properties and mass–radius scalings come from.

C.3.1. Structural Diversity—from Coreless to Mercury-structured Planets

The rocky planets of our own solar system, as well as exoplanets (e.g., Corot 7b), admit that rocky planets can have arbitrary core sizes. We focus on three planetary structures differing in core-to-planet mass fraction (or core mass fraction, f_c): (1) Earth-like structures with $f_c = 0.326$, (2) Mercury-structured with thin mantles and $f_c = 0.65$, and (3) coreless planets with $f_c \approx 0$. To generate our figures, we also modeled six intermediate core mass fraction values between our three major study cases. Each structure (average planetary and core radii $R_p(M)$, $R_c(M)$) can be described with individual mass–radius scalings, where M is the relative planet mass in Earth mass units:

$$R_p(M) = aM^{\phi}R_{p,\oplus} \quad (17)$$

$$R_c(M) = bM^{\psi}R_{c,\oplus}. \quad (18)$$

The parameters (a, b, ϕ, ψ) depend on core mass fraction, as well as on mantle and core composition (Table 1). We treat structural and compositional changes independent from each other because compositional changes do not, for our purposes, significantly affect mass–radius scalings (for Fe/Mg and $MgO/MgSiO_3$ ratios varying within ~50% the difference in $R_p(M)$ is <10%; see, e.g., Valencia et al. 2006; Seager et al. 2008). Hence, we focus on mass–radius scaling parameters (a, b, ϕ, ψ) only depending on core mass fraction f_c assuming an Earth-like Fe/Mg and $MgO/MgSiO_3$ mantle ratio and core composition. We assume average mantle and core densities $\rho_m(M)$, $\rho_c(M)$:

$$\rho_m(M) = 3M_p(1 - f_c)[4\pi(R_p^3 - R_c^3)]^{-1},$$
$$\rho_c(M) = 3(4\pi)^{-1}M_p f_c R_c^{-3}. \quad (19)$$

Gravity is generally considered constant throughout the mantle of each planet (Wagner et al. 2011) and thus approximated by the surface gravity $g_0(M)$ (with $G = 6.673 \times 10^{-11}\,{\rm m^3\,kg^{-1}\,s^{-2}}$):

$$g(M) \approx g_0(M) = GM_pR_p^{-2}. \quad (20)$$

For small cores, gravity significantly varies with mantle depth, and Equation (20) is not generally valid. However, we find no significant impact of depth-dependent gravity on our results for $V_{\rm eff}^* \sim 0$ because the lower mantle heat flux quickly adjusts to a change in gravity after a few hundred Myr (not valid for $V_{\rm eff}^* \gg 0$; see Section B.2).

C.3.2. Compositional Variation—from Earth to Carbon Planets

To determine the compositional parameter limits of our study, we combine literature results on thermal and transport properties for dry and wet silicates, oxides, SiC, and C rocks, the Dulong-Petit law, thermodynamic relations (e.g., in Stamenković et al. (2011), Section 4.1 and Equation (24)), and the evolution of the ISM. This knowledge results in the following approximate and broad compositional parameter range in relation to Earth reference values ("⊕") that we test: we use an initial radiogenic mantle heat sources concentration [W kg^{-1}] of $0.1Q_{\oplus} \leqslant Q \leqslant 10Q_{\oplus}$, a reference mantle viscosity of $10^{-5}\eta_{\rm ref,\oplus} \leqslant \eta_{\rm ref} \leqslant 10^{9}\eta_{\rm ref,\oplus}$, an activation energy of $E_{\oplus}^* - 120\,{\rm kJmol^{-1}} \leqslant E^* \leqslant E_{\oplus}^* + 300\,{\rm kJmol^{-1}}$, a mantle thermal conductivity of $0.5k_{m,\oplus} \leqslant k_m \leqslant 10k_{m,\oplus}$, a mantle thermal expansivity of $0.1\alpha_{m,\oplus} \leqslant \alpha_m \leqslant 2\alpha_{m,\oplus}$, mantle specific heats (at constant pressure) of $0.5\,C_{m,\oplus} \leqslant C_m \leqslant 2\,C_{m,\oplus}$ and lithospheric friction coefficients of $0.1C_{fric,\oplus} \leqslant C_{fric} \leqslant 10C_{fric,\oplus}$.

We must bear in mind that the only part of our parameter space that we can, from an order of magnitude perspective, uniquely associate with specific compositions, are the silicate and carbon planet domains (C.3.2.4), which are the focus of this paper. We discuss the remaining phase space in Section 4.2.3.

C.3.2.1. Initial Radiogenic Heat Sources

Estimates of how the ISM's concentration of radiogenic heat concentration evolved since the big bang suggest a variation of about two orders of magnitude of the initial radiogenic heat source concentration (in W kg^{-1}) decreasing with time of planet formation after the big bang—with Earth's radiogenic concentration roughly in the middle (e.g., Clayton 1988; Timmes et al. 1995; Gonzalez & Brownlee 2001). We use McDonough & Sun (1995) for our Earth reference case $Q_{\oplus}(t)$. We fix the Earth-like ratios of Th, K, and U and scale the total power output per kg. Additional effects might occur when this ratio varies.

C.3.2.2. Iron-rich and Wet Mantle Rock

Mineralogically bound iron impacts mostly mantle viscosity, thermal conductivity, rock density, and melting temperatures.

As we showed in Stamenković et al. (2011), effects on the thermal conductivity (and density) are of secondary importance (total thermal conductivity reduced by iron by a maximum of ∼15% and controlled by ferric iron Fe^{3+}, which quickly decreases with increasing pressure and hence planet depth), and the major effect of Fe on the evolution of planet interiors is via its impact on the viscosity. We follow Zhao et al. (2009), where Fe concentration reduces mantle viscosity and activation energy by maximally a factor of $\max(\partial\eta_{\rm ref}) \sim 1000$ and $\max(\Delta E^*) \sim 45$ kJ mol^{-1} from forsterite to fayalite. In this first order-of-magnitude study, we assume that iron impacts higher-pressure phases and other rock compositions similarly as for peridotite.

For wet mantle rock, we assume a reference viscosity reduction by two orders of magnitude, an activation energy reduction of 60 kJ mol^{-1}, and a possible reduction of the thermal conductivity by up to a factor of two (Karato 2008; Thomas et al. 2012). This assumption on wet mantle rock is only used to define the tested parameter space; the exact values have no impact on the qualitative results, as we did not study how water impacts plate tectonics.

C.3.2.3. Lithospheric Friction Coefficients

We vary lithospheric friction coefficients between $0.1C_{\rm fric,\oplus} \leqslant C_{\rm fric} \leqslant 10C_{\rm fric,\oplus}$. This results from experimental values for pure Al and Co, which are generally larger than one (up to ∼1.5) and values as small as 0.01 for strong surface water lubrication (Iaffaldano 2012). We assume a reference value for Earth of ∼0.15 for hydrated serpentines, which lies approximately in the middle of the currently known friction coefficient spectrum.

C.3.2.4. Silicate versus Carbon Planets

For a varying mantle iron and water concentration of 0%–100%, we can approximately describe silicate plants with all $\{E^*, \eta_{\rm ref}\}$ values smaller than or equal to the reference Earth values of $\{\{E^*, \eta_{\rm ref}\}: \{E^*, \eta_{\rm ref}\} \leqslant \{E^* = 300\,{\rm kJ\,mol^{-1}}, \eta_{\rm ref} = 10^{21}\,{\rm Pa\,s}\}\}$, a thermal conductivity of $0.5k_{m,\oplus}-1k_{m,\oplus}$, and thermal expansivity and specific heat corresponding to the Earth reference values (see Table 1). However, including even larger variations in thermal conductivity, expansivity, and heat capacity for silicate planets (we tested variations up to a factor of two in relation to Earth reference values) has no significant impact on our qualitative results for silicate planets, which are mainly controlled by the rheology.

For carbon planets, the currently most reliable order-of-magnitude estimate to understand in what approximate way the thermal evolution of carbon planets might differ from Earth-like oxide-dominated planets is by assuming that SiC, graphite, and diamond are the major interior constituents of their mantles. We focus on SiC as the most likely major upper mantle constituent (most crucial zone for plate tectonics). Moreover, the currently available data for diamond indicate similar trends as for SiC for rheology and thermal conductivity.

We use currently available order-of-magnitude estimates for viscosity, thermal conductivity and expansivity, and heat capacity for SiC: experimentally and with ab initio calculations, Ghoshtagore & Coble (1966), Koga et al. (2005), Kröger et al. (2003), and Rüschenschmidt et al. (2004) find that self-diffusion enthalpies of Si and C in SiC (also in diamond) are on the order of $E^* \sim 600$ kJ mol^{-1}, whereas the pre-exponential factor D_0 is of similar magnitude as for Si and Mg diffusion in perovskites (compare with Dobson et al. 2008; Stamenković et al. 2011). The diffusivity $D \sim D_0 \exp(-E^*/(R_g T))$ is inversely proportional to the rock viscosity $\eta \sim D^{-1}$ and is majorly controlled by the (effective) activation energy E^* (variation between carbon and silicate rocks in density, grain size, grain size dependence, and average molecular weight and pre-exponential constants are of secondary importance and neglected in this first study). We find the reference viscosity to be about $\sim\exp((E^*_C - E^*_\oplus)R_g^{-1}T_{\rm ref}^{-1}) \sim 5 \times 10^9$ times larger than the reference viscosity for Earth rocks being $\eta_{\rm ref,SiC} \sim 10^{30}$ Pa s (for $T_{\rm ref} = 1600$ K). Thermal expansivity and conductivity, as well as heat capacity values for SiC from the experiments by Goldberg et al. (2001) and Nilsson et al. (1997), are compared with our predictions for Earth-like rock from Stamenković et al. (2011), leading to an about one order of magnitude larger thermal conductivity and one order of magnitude smaller thermal expansivity in relation to silicates and oxides ($k_{m,\rm SiC} \sim 10k_{m,\oplus}$, $C_{m,\rm SiC} \sim C_{m,\oplus}$, $\alpha_{m,\rm SiC} \sim 0.1\alpha_{m,\oplus}$) (the Dulong–Petit law leads to almost identical heat capacity values for SiC as for $MgSiO_3$). Altogether, this leads for carbon planets approximately to $(E^*, \eta_{\rm ref}, k_m, \alpha_m, C_m)|_{\rm SiC} = (600\,{\rm kJ\,mol^{-1}}, 10^{30}\,{\rm Pa\,s}, 40\,{\rm Wm^{-1}\,K^{-1}}, 2\times10^{-6}{\rm K^{-1}}, C_{m,\oplus})$.

In this first work, we do not account for water and iron impacts within the carbon planet domain, as we are interested in a first glimpse into pure carbon planets.

Carbon-induced changes in mass–radius scalings have only minor effects on our results and are thus not considered. Also, the impact of an SiC chemistry on friction coefficients is hard to estimate, but we do expect that the differences between carbon and silicate planets are controlled by the many order-of-magnitude differences in viscosity and thermal conductivity.

C.3.3. Initial Interior Temperatures—from Adiabatic to Molten

Initial interior temperatures modulate the evolution of plate tectonics with time but are uncertain. We thus allow a large uncertainty in initial conditions from initially "cool" to initially "hot" planets. The initially "cool" planet scenario uses (most likely significantly underestimated; see Stamenković et al. 2012; Tackley et al. 2013) interior temperatures commonly found in literature (i.e., Valencia et al. 2006; Papuc & Davies 2008). This "cool" scenario is based on adiabatic temperatures across the mantle with an upper initial interior temperature of $T_{\rm m}(0) \sim 1700$ K, which leads, depending on planet size and structure, to initial core-mantle-boundary (CMB) temperatures of $T_{\rm c}(0) \sim 3900$ K for Earth and 6100 K for a 10 $M_\oplus$ Earth-like-structured planet (see Table 1 in Stamenković & Breuer 2014). The initially "hot" scenario mimics a planet with initial interior temperatures right below the solidus (so forming molten), which is more plausible (see, e.g., Breuer & Moore 2015). Note that we are not modeling the transition from melt to solid but start right below the solidus for the "hot" scenario. The adopted melting temperatures are based on Stamenković et al. (2011) for the deep mantle (supported by experiments; McWilliams et al. 2012) and for the upper mantle on an interpolation of collected experimental data (Zerr et al. 1998; Herzberg et al. 2000; Fiquet et al. 2010). For this "hot" initial scenario and $M_p \geqslant M_\oplus$, we obtain initial temperatures from 1700–2300 K in the upper mantle to 5100–20,000 K at the planet's CMB (depending on CMB pressure and hence on planet mass and structure).

REFERENCES

Badro, J., Fiquet, G., Guyot, F., et al. 2003, Sci, 300, 789
Badro, J., Rueff, J.-P., Vankó, G., et al. 2004, Sci, 305, 383
Bergemann, M., Ruchti, G. R., Serenelli, A., et al. 2014, A&A, 565, 11
Bond, J. C., O'Brien, D. P., & Lauretta, D. S. 2010, ApJ, 715, 1050
Breuer, D., & Moore, W. B. 2015, Planets and Moons: Dynamics and Thermal History of the Terrestrial Planets, the Moon, and Io (Amsterdam: Elsevier)
Buchhave, L. A., Bizzarro, M., Latham, D. W., et al. 2014, Natur, 509, 593
Buchhave, L. A., Latham, D. W., Johansen, A., et al. 2012, Natur, 486, 375
Buffett, B. A., Huppert, H. E., Lister, J. R., & Woods, A. W. 1996, JGR, 101, 7989
Byerlee, J. D. 1968, JGR, 73, 4741
Chorost, M. 2013, Astronomy Now, June 2013, 18
Clayton, D. D. 1988, MNRAS, 234, 1
Demory, B. O., Gillon, M., de Wit, J., et al. 2016, Natur, 532, 207
Deschamps, F., & Sotin, C. 2000, GeoJI, 143, 204
Dobson, D. P., Dohmen, R., & Wiedenback, M. 2008, E&PSL, 270, 125
Driscoll, P., & Olson, P. 2011, Icar, 213, 12
Escartin, J., Hirth, G., & Evans, B. 2001, Geo, 29, 1023
Fiquet, G., Auzende, A. L., Siebert, J., et al. 2010, Sci, 329, 1516
Foley, B. J., Bercovici, D., & Landuyt, W. 2012, E&PSL, 331, 281
Gaidos, E., Conrad, C. P., Manga, M., & Herlund, J. 2010, ApJ, 718, 596
Ghiorso, M. S. 2004, AmJS, 304, 752
Ghoshtagore, R. N., & Coble, R. L. 1966, PhRv, 143, 623
Gillon, M., Jehin, E., Lederer, S. M., et al. 2016, Natur, 533, 221
Goldberg, Y., Levinshtein, M. E., & Rumyantsev, S. L. 2001, in In Properties of Advanced Semiconductor Materials GaN, AlN, SiC, BN, SiC, SiGe, ed. M. E. Levinshtein, S. L. Rumyantsev, & M. S. Shur (New York: Wiley)
Gonzalez, G., & Brownlee, D. 2001, Icar, 152, 185
Grott, M., & Breuer, D. 2008, Icar, 193, 503
Grott, M., Breuer, D., & Laneuville, M. 2011, E&PSL, 307, 135
Herzberg, C., Raterron, P., & Zhang, J. 2000, GGG, 1, 1051
Höink, T., & Lenardic, A. 2010, GeoJI, 180, 23
Höink, T., Lenardic, A., & Richards, M. A. 2012, GeoJI, 191, 30
Hüttig, C., & Stemmer, K. 2008, PEPI, 171, 137
Iaffaldano, G. 2012, E&PSL, 357, 21
Jellinek, A. M., & Jackson, M. G. 2015, NatGe, 8, 587
Karato, S.-I. 2008, Deformation of Earth Materials: An Introduction to the Rheology of Solid Earth (London: Cambridge Univ. Press)
Karato, S.-I. 2011, Icar, 212, 14
Koga, K. T., Walter, M. J., Nakamura, W., & Kobayashi, K. 2005, PhRvB, 72, 024108
Korenaga, J. 2003, GeoRL, 30, 1437
Korenaga, J. 2010, ApJL, 725, 43
Kröger, H., Ronning, C., Hofsäss, H., et al. 2003, Diamons and Related Materials, 12, 2042
Kuchner, M., & Seager, S. 2005, arXiv:astro-ph/0504214
Lenardic, A., & Crowley, J. 2012, ApJ, 755, 132
Madhusudan, N., Lee, K. M., & Mousis, O. 2012, ApJL, 759, 5
McDonough, W. F., & Sun, S.-S. 1995, ChGeo, 120, 223
McWilliams, R. S., Spaulding, D. K., Eggert, J. H., et al. 2012, Sci, 338, 1330
Moresi, L., & Solomatov, V. 1998, GeoJI, 133, 669
Nilsson, O., Mehling, H., Horn, R., et al. 1997, HTHP, 29, 73
Noack, L., & Breuer, D. 2014, P&SS, 98, 41
O'Neill, C., Jellinek, A. M., & Lenardic, A. 2007, E&PSL, 261, 20
O'Neill, C., & Lenardic, A. 2007, GeoRL, 34, L19204
O'Rourke, J. G., & Korenaga, J. 2012, Icar, 221, 1043
Papuc, A., & Davies, G. F. 2008, Icar, 195, 447
Ramirez, I., Allende Prieto, C., & Lambert, D. L. 2013, ApJ, 764, 78
Richards, M., Yang, W.-S., Baumgardner, J. R., & Bunge, H.-P. 2001, GGG, 2, 1026
Rüschenschmidt, K., Bracht, H., Stolwijk, N. A., et al. 2004, JAP, 96, 1458
Seager, S., Bains, W., & Hu, R. 2013, ApJ, 775, 104
Seager, S., Kuchner, M., Hier-Majumder, C. A, & Militzer, B. 2008, ApJ, 669, 1279
Solomatov, V. S. 2004, JGR, 109, B01412
Sotin, C., Grasset, O., & Mocquet, A. 2007, Icar, 191, 337
Sotin, C., & Labrosse, S. 1999, PEPI, 112, 171
Stamenković, V., & Breuer, D. 2014, Icar, 234, 174
Stamenković, V., Breuer, D., & Spohn, T. 2011, Icar, 216, 572
Stamenković, V., Lenardic, A., & Höink, T. 2016, JGRE, 121, 4994
Stamenković, V., Noack, L., Breuer, D., & Spohn, T. 2012, ApJ, 748, 41
Stamenković, V., & Sohl, F. 2015, in Encyclopedia of Astrobiology, Part 19, ed. M. Gargaud et al. (Berlin: Springer), 1452
Stein, C., Finnenkötter, A., Lowman, J. P., & Hansen, U. 2011, GeoRL, 38, L21201
Stein, C., Lowman, J. P., & Hansen, U. 2013, E&PSL, 361, 448
Stein, C., Schmalzl, J., & Hansen, U. 2004, PEPI, 142, 225
Stevenson, D. J., Spohn, T., & Schubert, G. 1983, Icar, 54, 466
Tachinami, C., Senshu, H., & Ida, S. 2011, ApJ, 726, 1
Tackley, P. 2000, GGG, 1, 1
Tackley, P. J., Ammann, M., Brodholt, J. P., Dobson, D. P., & Valencia, D. 2013, Icar, 225, 50
Thomas, S. M., Bina, C. R., Jacobsen, S. D., & Goncharov, A. F. 2012, E&PSL, 357, 130
Timmes., F. X., Wooslet, S. E., & Weaver, T. A. 1995, ApJS, 98, 617
Tozer, D. C. 1967, in The Earth's Mantle, ed. T. F. Gaskell (London: Academic), 325
Trompert, R., & Hansen, U. 1998, Natur, 395, 686
Turcotte, D. L., & Schubert, G. 2002, Geodynamics (2nd ed.; Cambridge: Cambridge Univ. Press)
Valencia, D., O'Connell, R. J., & Sasselov, D. 2006, Icar, 181, 545
Valencia, D., O'Connell, R. J., & Sasselov, D. D. 2007, ApJL, 670, 45
Van Heck, H. J., & Tackley, P. J. 2011, E&PSL, 310, 252
Wagner, F. W., Sohl, F., Hussmann, H., Grott, M., & Rauer, H. 2011, Icar, 214, 366
Wong, T., & Solomatov, V. S. 2015, PESS, 2, 18
Yamazaki, D., & Karato, S.-I. 2001, AmMin, 86, 385
Zerr, A., Diegler, A., & Boehler, R. 1998, Sci, 281, 243
Zhao, Y.-H., Zimmermann, M. E., & Kohlstedt, D. L. 2009, E&PSL, 287, 229